STABILITY AND BIFURCATION OF PREDATOR-PREY MODELS WITH THE ALLEE EFFECT

SİNAN KAPÇAK

JULY 2013

STABILITY AND BIFURCATION OF PREDATOR-PREY MODELS WITH THE ALLEE EFFECT

A DISSERTATION SUBMITTED TO

THE GRADUATE SCHOOL OF NATURAL

AND APPLIED SCIENCES OF

IZMIR UNIVERSITY OF ECONOMICS

BY

SİNAN KAPÇAK

IN PARTIAL FULFILLMENT OF THE REQUIREMENTS

FOR THE DEGREE OF DOCTOR OF PHILOSOPHY

IN THE GRADUATE SCHOOL OF NATURAL AND APPLIED SCIENCES

JULY 2013

Ph.D. DISSERTATION EXAMINATION RESULT FORM

Approval of the Graduate School of Natural and Applied Sciences

Prof. Dr. Murat Aşkar
Director

I certify that this thesis satisfies all the requirements as a thesis for the degree of Doctor of Philosophy.

Prof. Dr. İsmihan Bayramoğlu
Head of Department

We have read the dissertation entitled **"Stability and Bifurcation of Predator-prey Models with the Allee Effect"** completed by **SİNAN KAPÇAK** under supervision of **Prof. Dr. Ünal Ufuktepe** and **Prof. Dr. Saber Elaydi** and we certify that in our opinion it is fully adequate, in scope and in quality, as a dissertation for the degree of Doctor of Philosophy.

Prof. Dr. Saber Elaydi
Co-Supervisor

Prof. Dr. Ünal Ufuktepe
Supervisor

Examining Committee Members

Date: 07.15.2013

Prof. Dr. Ünal Ufuktepe
Dept. of Mathematics, İUE

Prof. Dr. Murat Adıvar
Dept. of Mathematics, İUE

Prof. Dr. Necdet Bildik
Dept. of Mathematics, CBU

Prof. Dr. Ferit Acar Savacı
Dept. of Elec. and Elec. Eng., IZTECH

Assoc. Prof. Dr. Serap Topal
Dept. of Mathematics, EU

ABSTRACT

STABILITY AND BIFURCATION OF PREDATOR-PREY MODELS WITH THE ALLEE EFFECT

SİNAN KAPÇAK
Ph.D. in Applied Mathematics and Statistics
Graduate School of Natural and Applied Sciences
Supervisor: Prof. Dr. Ünal Ufuktepe
Co-Supervisor: Prof. Dr. Saber Elaydi
July 2013

One of the most well-known model with several interacting populations is Nicholson-Bailey host-parasitoid model [44]. This is a nonlinear discrete-time model to a biological system involved two insects, a parasitoid and its host. Beddington et al investigated a density-dependent version of Nicholson-Bailey model where the host rate of increase is logistic [4]. Another more realistic version of the system was studied by Hone, Irle, and Thurura where the model displays the more biologically relevant possibilities that the two populations can asymtotically approach positive steady-state values or move towards an attracting invariant curve in the phase plane [21].

This thesis will investigate the generalization of Beddington model and the Beddington model with Allee effect.

Keywords: discrete dynamical systems, beddington model, allee effect, stability, invariant curves, bifurcation.

ÖZ

AV-AVCI MODELLERİNİN ALLEE ETKİSİ ALTINDA STABİLİTE VE DALLANMASI

SİNAN KAPÇAK
Uygulamalı Matematik ve İstatistik, Doktora
Fen Bilimleri Enstitüsü
Tez Danışmanı: Prof. Dr. Ünal Ufuktepe
İkinci Tez Danışmanı: Prof. Dr. Saber Elaydi
Temmuz 2013

Birbirinden farklı popülasyonların etkileşiminin en iyi bilinen örneklerinden biri Nicholson-Bailey konakçı-parazitoid modelidir [44]. Bu, bir parazitoid ve konakçısından oluşan, doğrusal olmayan bir kesikli-zaman modelidir. Beddington ve arkadaşları, Nicholson-Bailey modelinin, konakçı sayısının lojistik olarak büyüdüğü, yoğunluğa bağlı versiyonunu araştırmışlardır [4]. Yine aynı sistemin gerçekçi başka bir hali Hone, Irle ve Thurura tarafından modellenmiştir. Bu modelde, faz düzleminde, iki popülasyon da asimtotik olarak sabit noktalara veya invaryant bir eğriye yakınsayabiliyor [21].

Bu tezde, Beddington modelinin genelleştirilmiş halini ve bu modelin Allee etkisi altındaki dinamiklerini araştıracağız.

Anahtar Kelimeler: kesikli dinamik sistemler, beddington modeli, allee etkisi, stabilite, invaryant eğriler, dallanma.

ACKNOWLEDGEMENT

I would like to express my very great appreciation to Prof. Dr. Ünal Ufuktepe for his patient guidance, enthusiastic encouragement and useful critiques of this Ph.D. thesis. He is not only supervisor but dear friend. His positive outlook and confidence in my research inspired me and gave me confidence. I would like to express my heartfelt gratitude to my co-supervisor Prof. Dr. Saber Elaydi for his help and support during this research and my visit to Trinity University, TX, U.S.A. His willingness to give his time so generously has been very much appreciated.

I would like to express my appreciation to the advice of the committee members, Prof. Dr. Murat Adıvar and Assoc. Prof. Dr. Serap Topal, for their critical comments, which enabled me to notice the weaknesses of my dissertation and make the necessary improvements according to their comments.

I would like to acknowledge the academic support of İzmir University of Economics, in the award of a Postgraduate Studentship. My sincere thanks go to The Scientific & Technological Research Council of Turkey (TÜBITAK) for their financial support for my visit to Trinity University. I would also like to thank Trinity University for hosting me during the period the part of this thesis was written.

Special thanks should be given to my dear friends Assoc. Prof. Gözde Yazgı Tütüncü, Göknur Giner, Gülder Kemalbay, Nalan Gündüz, Abdulkadir Doğru, Uğur Akduman, Savaş Yücel, and my cousins Emre Bostan, Elif Esra Döm, and Veysel Bilge for their support and encouragement.

Last but not least, I am greatly indebted to my family who form the backbone and origin of my happiness. Their love and support without any complaint or

regret has enabled me to complete this Ph.D. research.

To my family

TABLE OF CONTENTS

LIST OF TABLES

LIST OF FIGURES

Chapter 1

Introduction

The qualitative analysis of nonlinear dynamical systems has become increasingly widespread in physics and have been used in theoretical ecology since the beginning of the last century. The dynamical relationship between predators and their prey is one of the dominant themes in ecology. Alfred John Lotka (1880-1949) and Vito Volterra (1860-1946), the most prominent founders of mathematical ecology, investigated the dynamics of interacting populations [38], [50]. Hofbauer and Sigmund [19] offer an extended treatment of a generalized version of the predator-prey model. The variations of predator-prey models can be found in [41].

The Nicholson-Bailey model [44] which is a discrete model of the interaction between a predator P and a prey N, where it is assumed that the predator can consume the prey without limit, is given by

$$\begin{aligned} N_{t+1} &= rN_t \exp(-aP_t), \\ P_{t+1} &= eN_t(1 - \exp(-aP_t)), \end{aligned} \tag{1.1}$$

where the parameters $r, a, e > 0$. The model is unrealistic in the sense that solutions can grow unboundedly with t [42]. Beddington et al [4] investigated a density-dependent predator-prey model where the host rate of increase is logistic:

$$\begin{aligned} N_{t+1} &= N_t \exp\left[r\left(1-\frac{N_t}{K}\right)-aP_t\right], \\ P_{t+1} &= eN_t(1-\exp(-aP_t)) \end{aligned} \tag{1.2}$$

where K is the carrying capacity.

Hone, Irle, and Thurura [21] has studied the following predator-prey system which is the more general form of the system (1.1):

$$\begin{aligned} N_{t+1} &= rN_t \exp(-aP_t), \\ P_{n+1} &= eN_t(1-\exp(-bP_t)). \end{aligned} \tag{1.3}$$

The main goal of this thesis is to investigate the following density-dependent predator-prey model, which is the generalization of models (1.1), (1.2), and (1.3):

$$\begin{aligned} N_{t+1} &= N_t \exp\left[r\left(1-\frac{N_t}{K}\right)-aP_t\right], \\ P_{t+1} &= eN_t[1-\exp(-bP_t)], \end{aligned} \tag{1.4}$$

where the parameters r, K, a, b, e are positive.

In this thesis, we also discuss the stability analysis of the Beddington model with an Allee effect. The Allee effect is a phenomenon in biology characterized by a positive correlation between population size or density and the mean individual fitness of a population or species [1]. Although the concept of Allee effect had no title at the time, it was first described in the 1930s by its namesake, Warder Clyde Allee. Through experimental studies, Allee was able to demonstrate that goldfish grow more rapidly when there are more individuals within the tank [1]. This led him to conclude that aggregation can improve the survival rate of individuals, and that cooperation may be crucial in the overall evolution of social structure.

The classical view of population dynamics stated that due to competition for resources, a population will experience a reduced overall growth rate at higher density and increased growth rate at lower density. In other words, we would be better off when there are fewer of us around due to a limited amount of resources. However, the Allee effect concept introduced the idea that the reverse holds true when the population density is low. Individuals within a species generally require the assistance of another for more than simple reproductive reasons in order to persist. Examples of these can easily be seen in animals that hunt for prey or defend against predators as a group.

This thesis is organized as follows: A review of the basic theory of discrete dynamical systems and related population models are contained in Chapter 2. In Chapter 3, the concept of Allee effect and an example of a predator-prey model with Allee effect are presented. We investigate the stability analysis of the model. The main problem, namely, the generalized Beddington model is given in Chapter 4. The stability and bifurcation for the problem is investigated and the numerical computations are also confirm our results. We also discuss the stability analysis of the Beddington model with an Allee effect. In the last chapter, we present the final remarks and future work of our research.

Chapter 2

Preliminaries

2.1 Stability of Fixed Points for One-Dimesional Maps

Most of the definitions and the theorems given in this chapter are taken directly from [13], [35], [18], and [3].

Definition. Consider the difference equation

$$x_{n+1} = f(x_n). \tag{2.1}$$

A point x^* is said to be a **fixed** point of the map f or an **equilibrium** point of equation (2.1) if $f(x^*) = x^*$.

Closely related fixed points are the **eventually fixed points**. These are the points that reach a fixed point after finitely many iterations. More explicitely, a point x is said to be an **eventually fixed point** of a map f if there exist a positive integer r and a fixed point x^* of f such that $f^r(x) = x^*$, but $f^{r-1}(x) \neq x^*$, where $f^r = \underbrace{f \circ f \circ f \circ \cdots f \circ f}_{r \text{ compositions}}$.

The set of all fixed points is denoted by $Fix(f)$, the set of all eventually fixed points by $EFix(f)$, and the set of all eventually fixed points of the fixed point x^* by $EFix_{x^*}(f)$.

Theorem 2.1 *Let $f : I \to I$ be a continuous map, where $I = [a, b]$ is a closed interval in $\mathbb{R}$. Then, f has a fixed point.*

Theorem 2.2 *Let $f : I \to \mathbb{R}$ be a continuous map such that $f(I) \supset I$. Then f has a fixed point in I.*

Definition. Let $f : I \to I$ be a map and $x^* \in I$ be a fixed point of f, where I is an interval in the set of real numbers $\mathbb{R}$. Then

1. x^* is said to be **stable** if for any $\varepsilon > 0$ there exists $\delta > 0$ such that for all $x \in I$ with $|x - x^*| < \delta$ we have $|f^n(x) - x^*| < \varepsilon$ for all $n \in \mathbb{Z}^+$. Otherwise, the fixed point x^* will be called **unstable**.
2. x^* is said to be **attracting** if there exists $\eta > 0$ such that $|x - x^*| < \eta$ implies $\lim_{n\to\infty} f^n(x) = x^*$.
3. x^* is said to be **asymptotically stable** if it is both stable and attracting. If in (2) $\eta = \infty$, then x^* is said to be **globally asymptotically stable**.

Fixed points may be divided into two types: **hyperbolic** and **nonhyperbolic**. A fixed point x^* of a map f is said to be hyperbolic if $|f(x^*)| \neq 1$. Otherwise, it is nonhyperbolic.

Theorem 2.3 *Let x^* be a hyperbolic fixed point of a map f, where f is continuously differentiable at x^*. The following statements then hold true:*

1. *If $|f'(x^*)| < 1$, then x^* is asymptotically stable.*
2. *If $|f'(x^*)| > 1$, then x^* is unstable.*

Theorem 2.4 *Let x^* be a fixed point of a map f such that $f'(x^*) = 1$. If $f'(x)$, $f''(x)$, and $f'''(x)$ are continuous at x^*, then the following statements hold:*

1. *If $f''(x^*) \neq 0$, then x^* is unstable. Moreover, it is semistable from the right if $f''(x*) < 0$, and is semistable from left if $f''(x*) > 0$.*

2. *If $f''(x^*) = 0$ and $f'''(x^*) > 0$, then x^* is unstable.*

3. *If $f''(x^*) = 0$ and $f'''(x^*) < 0$, then x^* is asymptotically stable.*

Definition. The **Schwarzian derivative**, Sf, of a function f is defined by

$$Sf(x) = \frac{f'''(x)}{f'(x)} - \frac{3}{2}\left[\frac{f''(x)}{f'(x)}\right]^2.$$

And if $f'(x^*) = -1$, then

$$Sf(x^*) = -f'''(x^*) - \frac{3}{2}[f''(x^*)]^2.$$

Theorem 2.5 *Let x^* be a fixed point of a map f such that $f'(x^*) = -1$. If $f'(x)$, $f''(x)$, and $f'''(x)$ are continuous at x^*, then the following statements hold:*

1. *If $Sf(x^*) < 0$, then x^* is asymptotically stable.*

2. *If $Sf(x^*) > 0$, then x^* is unstable. Moreover, it cannot be semistable.*

2.2 Stability of Fixed Points for Two-Dimensional Maps

Definition. A fixed point X^* of a map $f : \mathbb{R}^2 \to \mathbb{R}^2$ is said to be

1. **stable** if given $\varepsilon > 0$ there exists $\delta > 0$ such that $|X - X^*| < \delta$ implies $|f^n(X) - X^*| < \varepsilon$ for all $n \in \mathbb{Z}^+$.

2. **attracting** (sink) if there exists $\nu > 0$ such that $|X - X^*| < \nu$ implies $\lim_{n\to\infty} f^n(X) = X^*$. It is **globally attracting** if $\nu = \infty$.

3. **asymptotically stable** if it is both stable and attracting. It is **globally asymptotically stable** if it is both stable and globally attracting.

Theorem 2.6 *Consider the system of difference equations*

$$X_{n+1} = AX_n \tag{2.2}$$

where A is a 2×2 matrix. Denote $\rho(A) = \max\{|\lambda_1|, |\lambda_2|\}$ where λ_1 and λ_2 are the eigenvalues of the matrix A. The following statements hold for the equation (2.2).

(a) If $\rho(A) < 1$, then the origin is asymptotically stable.

(b) If $\rho(A) > 1$, then the origin is unstable.

(a) If $\rho(A) = 1$, then the origin is unstable if the Jordan form is of the form $\begin{pmatrix} \lambda & 1 \\ 0 & \lambda \end{pmatrix}$, and stable otherwise.

Lemma 2.7 *Let x_1 and x_2 be the roots of the equation $x^2 - tx + d = 0$ where t and d are real numbers. Then $|x_1| < 1$ and $|x_2| < 1$ if and only if*

$$|t| < 1 + d < 2.$$

Proof. The roots can be both real or complex conjugates:

Case 1. Let the roots be complex conjugates: $a+ib$ and $a-ib$. Then $x_1+x_2 = 2a = t$ and $x_1x_2 = a^2 + b^2 = d$.

$\Rightarrow$: Since $|x_1| < 1$ and $|x_2| < 1$, $a^2 + b^2 < 1$ is always true. We will show that $|t| < 1 + d < 2$.

For the first inequality $|t| < 1+d$, since $a^2-2|a|+1+b^2 > 0$, $|2a| < 1+a^2+b^2$. For the second inequality, we have $a^2 + b^2 < 1$, which we already know.

$\Leftarrow$: By our assumption $|2a| < 1 + a^2 + b^2 < 2$ we have $a^2 + b^2 < 1$. Thus, $|x_1| = |x_2| = \sqrt{a^2 + b^2} < 1$.

Case 2. Now, let the roots be real.

$\Rightarrow$: Since $|x_1| < 1$ and $|x_2| < 1$, we have $0 < (1-x_1)(1-x_2) = 1 - x_1 - x_2 + x_1x_2$ from which we get $x_1 + x_2 < 1 + x_1x_2$. Similarly, using the fact that $0 < (1+x_1)(1+x_2)$, we get $-(x_1+x_2) < 1 + x_1x_2$. Combining these two inequalities, we obtain $|x_1 + x_2| < 1 + x_1x_2$. The second part of the inequality is obvious.

$\Leftarrow$: We assume that $|x_1 + x_2| < 1 + x_1x_2$ and $x_1x_2 < 1$ which yields

$$-1 - x_1x_2 < x_1 + x_2 < 1 + x_1x_2$$

or

$$-(1+x_1)(1+x_2) < 0 < (1-x_1)(1-x_2).$$

Thus, we have

$$(1-x_1)(1-x_2) > 0,$$
$$(1+x_1)(1+x_2) > 0.$$

By the assumption, we also have that $x_1x_2 < 1$.

If $|x_1| \geq 1$ or/and $|x_2| \geq 1$, then at least one of the conditions above can not be satisfied. Further, $|x_1| < 1$ and $|x_2| < 1$ satisfy the conditions above.

□

Hence, we have the following theorem:

Theorem 2.8 *In equation (2.2), the origin is asymptotically stable if the following condition holds true:*

$$|trA| - 1 < \det A < 1.$$

In Appendix B, Table B.1, B.2, and B.3 represent some trace and determinant values in the Trace-Determinant plane, their corresponding eigenvalues, and the orbits of a linear system in the phase diagram. On the column **Eigenvalues**, two dots represent the eigenvalues on the complex plane with the unit circle. The phase diagram of the linear system with the corresponding eigenvalues is given on the column **Phase Plane**. The black dot represents the final point after 100 iterations.

On the column **Tr-Det Diagram**, if the point is in the region given by the Theorem 2.8, then the system is stable. Hence, the eigenvalues are inside the unit circle and final point is at the origin. If the point is outside the region given by the Theorem 2.8, then the system is unstable. So, the eigenvalues are outside the unit circle and final point is far from the origin.

2.3 Invariant Manifolds

In this section, the appropriate tools that allows us to compute the center manifolds and the stable and unstable manifolds are presented [18], [13].

Let $F : \mathbb{R}^k \to \mathbb{R}^k$ be a map such that $F \in C^2$ and $F(0) = 0$. Then one may write F as a perturbation of a linear map L,

$$F(X) = LX + R(X)$$

where L is a $k \times k$ matrix defined by $L = D(F(0))$, $R(0) = 0$, and $DR(0) = 0$, where D denotes the derivative. Now we will introduce special subspace of $\mathbb{R}^k$, called invariant manifolds [53].

An invariant manifold is a manifold embedded in its phase space with the property that it is invariant under the dynamical system generated by F. A subspace M of $\mathbb{R}^k$ is an invariant manifold if whenever $X \in M$, then $F^n(X) \in M$, for all $n \in \mathbb{Z}^+$. For the linear map L, one may split its spectrum $\sigma(L)$ into three sets σ_s, σ_u, and σ_c, for which $\lambda \in \sigma_s$ if $|\lambda| < 1$, $\lambda \in \sigma_u$ if $|\lambda| > 1$, and $\lambda \in \sigma_c$ if $|\lambda| = 1$.

Corresponding to these sets, we have three invariant manifolds (linear subspaces) E^s, E^u, and E^c which are the generalized eigenspaces corresponding to σ_s, σ_u, and σ_c, respectively.

The main question is how to extend this linear theory to nonlinear maps. Corresponding to the linear subspaces E^s, E^u, and E^c, we will have the invariant manifolds the stable manifold W^s, the unstable manifold W^u, and the center manifold W^c.

The center manifolds theory is interesting only if $W^u = \{0\}$. In this case, the dynamics on the center manifold W^c determines the dynamics of the system. The other interesting case is when $W^c = \{0\}$ and we have a saddle. For the center manifold theory we reference [6],[7],[32],[53],[40],[51].

Let $E^s \subset \mathbb{R}^s$, $E^u \subset \mathbb{R}^u$, and $E^c \subset \mathbb{R}^t$, with $s + u + t = k$. Then one may formally define the above-mentioned invariant manifolds as follows:

$$W^s = \{x \in \mathbb{R}^k : F^n(x) \to 0 \quad as \quad n \to \infty\},$$

$$W^u = \{x \in \mathbb{R}^k : F^n(x) \to 0 \quad as \quad n \to -\infty\}.$$

Since the stability on the center manifold is not a priori known, it is defined as a manifold of dimension t whose graph is tangent to E^c at the origin.

Theorem 2.9 (Invariant Manifolds Theorem) [23],[40] *Suppose that* $F \in C^2$. *Then there exist* C^2 *stable* W^s *and unstable* W^u *manifolds tangent to* E^s *and* E^u*, respectively, at* $X = 0$ *and* C^1 *center manifold* W^c *tangent to* E^c *at* $X = 0$. *Moreover, the manifolds* W^c, W^s, *and* W^u *are all invariant.*

2.3.1 Center Manifolds

In this section, we focus on the case when $\sigma_u = \emptyset$. Hence the eigenvalues of L are either inside the unit disc or on the unit disc. By suitable change of variables, one may represent the map F as a system of difference equation such as

$$\begin{aligned} x_{n+1} &= Ax_n + f(x_n, y_n), \\ y_{n+1} &= By_n + g(x_n, y_n). \end{aligned} \tag{2.3}$$

First we assume that all eigenvalues of $A_{t\times t}$ are on the unit circle and all the eigenvalues of $B_{s\times s}$ are inside the unit circle, with $t + s = k$. Moreover,

$$f(0,0) = 0, \quad g(0,0) = 0, \quad Df(0,0) = 0, \quad Dg(0,0) = 0.$$

Since W^c is tangent to $E^c = \{(x, y) \in \mathbb{R}^t \times \mathbb{R}^t : y = 0\}$, it may be represented locally as the graph of a function $h : \mathbb{R}^t \to \mathbb{R}^t$ such that

$$W^c = \{(x, y) \in \mathbb{R}^t \times \mathbb{R}^t : y = h(x), h(0) = 0, Dh(0) = 0, |x| < \delta \text{ for a sufficently small } \delta\}.$$

Furthermore, the dynamics restricted to W^c is given locally by the equations

$$x_{n+1} = Ax_n + f(x_n, h(x_n)), \quad x \in \mathbb{R}^t. \tag{2.4}$$

The main feature of equation (2.4) is that its dynamics determine the dynamics of equation (2.3). So if $x^* = 0$ is a stable, asymptotically stable, or unstable fixed point of equation (2.4), then the fixed point $(x^*, y^*) = (0, 0)$ of equation (2.3) possesses the corresponding property.

To find the map $y = h(x)$, we substitute for y in equation (2.3) and obtain

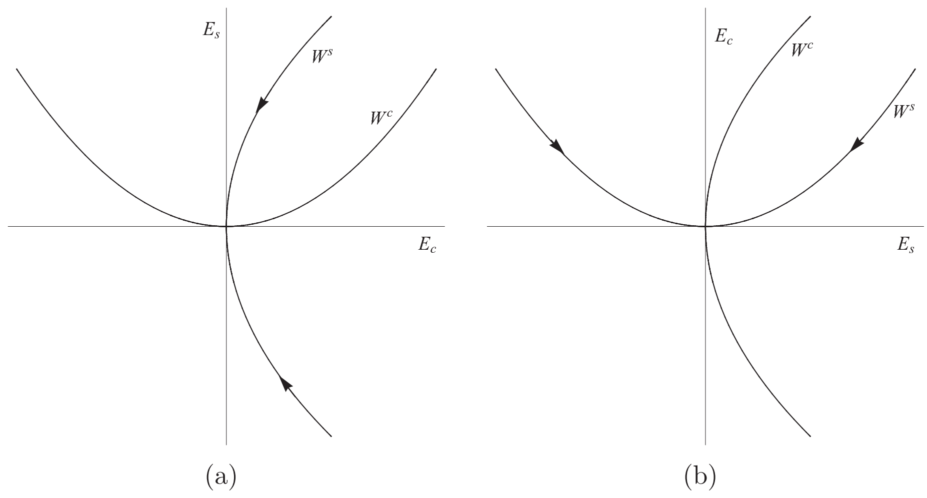

Figure 2.1: Stable and centre manifolds.

$$\begin{aligned} x_{n+1} &= Ax_n + f(x_n, h(x_n)), \\ y_{n+1} &= h(x_{n+1}) = h(Ax_n + f(x_n, h(x_n))). \end{aligned} \tag{2.5}$$

But

$$y_{n+1} = By_n + g(x_n, y_n) = Bh(x_n) + g(x_n, h(x_n)). \tag{2.6}$$

Equating (2.5) and (2.6) yields the center manifold equation

$$h[Ax_n + f(x_n, h(x_n))] = Bh(x_n) + g(x_n, h(x_n)). \tag{2.7}$$

Analogously if $\sigma(A) = \sigma_s$ and $\sigma(B) = \sigma_c$, one may define the center manifold W^c and obtain the equation

$$y_{n+1} = By_n + g(h(y_n), y_n),$$

where $x = h(y)$.

2.3.2 Stable and Unstable Manifolds

Suppose now that the map F is hyperbolic, that is $\sigma_c = \emptyset$. Then by Theorem 2.9, there are two unique invariant manifolds W^s and W^u tangent to E^s and E^u at $X = 0$, which are graphs of the maps

$$\varphi_1 : E_1 \to E_2 \quad \text{and} \quad \varphi_2 : E_2 \to E_1,$$

such that

$$\varphi_1(0) = \varphi_2(0) = 0 \quad \text{and} \quad D(\varphi_1(0)) = D(\varphi_2(0)) = 0.$$

Letting $y_n = \varphi_1(x_n)$ yields

$$y_{n+1} = \varphi_1(x_{n+1}) = \varphi_1(Ax_n + f(x_n, \varphi_1(x_n))).$$

But

$$y_{n+1} = B\varphi_1(x_n) + g(x_n, \varphi_1(x_n)).$$

Equating the two equations above yields

$$\varphi_1(Ax_n + C\varphi_1(x_n) + f(x_n, \varphi_1(x_n))) = B\varphi_1(x_n) + g(x_n, \varphi(x_n)), \tag{2.8}$$

where we can take, without loss of generality,

$$\varphi_1(x) = \alpha_1 x^2 + \beta_1 x^3 + O(|x|^4).$$

Similarly, letting $x_n = \varphi_2(y_n)$ yields

$$x_{n+1} = \varphi_2(y_{n+1}) = \varphi_2(By_n + g(\varphi_2(y_n), y_n)), \tag{2.9}$$

where we can take, without loss of generality,

$$\varphi_2(x) = \alpha_2 x + \beta_2 x^2 + O(|x|^3).$$

But

$$x_{n+1} = A\varphi_2(y_n) + Cy_n + f(\varphi_2(y_n), y_n), \tag{2.10}$$

and hence equating (2.9) and (2.10) then we get

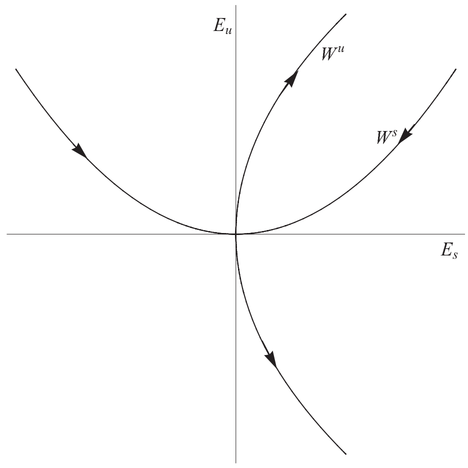

Figure 2.2: Stable and unstable manifolds.

$$\varphi_2(By_n + g(\varphi_2(y_n), y_n)) = A\varphi_2(y_n) + Cy_n + f(\varphi_2(y_n), y_n). \tag{2.11}$$

Using equations (2.8) and (2.11), one can find the stable manifold

$$W^s = \{(x, y) \in \mathbb{R}^t \times \mathbb{R}^t : y = \phi_1(x)\},$$

and the unstable manifold

$$W^u = \{(x, y) \in \mathbb{R}^t \times \mathbb{R}^t : x = \phi_2(y)\}.$$

2.4 Bifurcation

In this section, we present various types of changes in behaviour that can occur at bifurcation values. The types of bifurcations depend on how the dynamics of a map change as a single parameter is varied.

Consider a discrete-time dynamical system depending on a parameter

$$x \mapsto H(\mu, x), \quad x \in \mathbb{R}^n, \ \mu \in \mathbb{R},$$

where the map H is smooth with respect to both x and μ.

Let $x = x_0$ be a hyperbolic fixed point of the system for $\mu = \mu_0$. Let us monitor this fixed point and its eigenvalues while this parameter varies. It is clear that there are, generically, only three ways in which the hyperbolicity condition can be violated. Either a simple positive eigenvalue approaches the unit circle and we have $\lambda_1 = 1$, or a simple negative eigenvalue approaches the unit circle and we have $\lambda_1 = -1$, or a pair of simple complex eigenvalues reach the unit circle and we have $\lambda_{1,2} = e^{\pm i\theta_0}$, $0 < \theta_0 < \pi$, for some value of parameter. Now, we give the following definitions.

Definition. The bifurcation associated with the appearance of $\lambda_1 = 1$ is called a **fold** (or **tangent**) bifurcation.

This bifurcation is also referred to as a **limit point**, **saddle-node bifurcation**, **turning point**, among others.

Definition. The bifurcation associated with the appearance of $\lambda_1 = -1$ is called a **flip** (or **period doubling**) bifurcation.

Definition. The bifurcation corresponding to the presence of $\lambda_{1,2} = e^{\pm i\theta_0}$, $0 < \theta_0 < \pi$, is called a **Neimark-Sacker** (or **torus**) bifurcation [43], [46].

Notice that the fold and flip bifurcations are possible if $n \geq 1$, but for the Neimark-Sacker bifurcation we need $n \geq 2$.

Theorem 2.10 (The Saddle-node Bifurcation) *Suppose that* $H_\mu(x) \equiv H(\mu, x)$ *is a* C^2 *one-parameter family of one-dimensional maps. (i.e., both* $\frac{\partial^2 H}{\partial x^2}$ *and* $\frac{\partial^2 H}{\partial \mu^2}$ *exist and are continuous), and* x^* *is a fixed point of* H_{μ^*}*, with* $H'_{\mu^*}(x^*) = 1$*. Assume further that*

$$A = \frac{\partial H}{\partial \mu}(\mu^*, x^*) \neq 0 \quad \text{and} \quad B = \frac{\partial^2 H}{\partial x^2}(\mu^*, x^*) \neq 0.$$

Then there exists an interval I *around* x^* *and a* C^2 *map* $\mu = p(x)$*, where* $p : I \to \mathbb{R}$ *such that* $p(x^*) = \mu^*$*, and* $H_{p(x)}(x) = x$*. Moreover, if* $AB < 0$*, the fixed points exist for* $\mu > \mu^*$*, and if* $AB > 0$*, the fixed point exist for* $\mu < \mu^*$*.*

The proof of the above theorem can be found in [13]. For the proof, a version of Implicit Function Theorem is used. We state the theorem below:

Theorem 2.11 (The Implicit Function Theorem) *Suppose that* $G : \mathbb{R}\times\mathbb{R} \to \mathbb{R}$ *is a* C^1 *map in both variables such that for some* $(\mu^*, x^*) \in \mathbb{R}\times\mathbb{R}$, $G(\mu^*, x^*) = 0$ *and* $\frac{\partial G}{\partial \mu}(\mu^*, x^*) \neq 0$. *Then, there exists an open interval* J *around* μ^*, *an open interval* I *around* x^*, *and a* C^1 *map* $\mu = p(x)$, *where* $p : I \to J$ *such that*

1. $p(x^*) = \mu^*$.
2. $G(p(x), x) = 0$, *for all* $x \in I$.

Two types of bifurcation appear when $\frac{\partial H}{\partial x}(\mu^*, x^*) = 1$, but $\frac{\partial H}{\partial \mu}(\mu^*, x^*) = 0$: **transcritical bifurcation** and **pitchfork bifurcation**. In the Table 2.1, we give the conditions and related example for each types of bifurcation.

Theorem 2.12 (Period-doubling Bifurcation) *Suppose that*

1. $H_\mu(x^*) = x^*$ *for all* μ *in an interval around* μ^*.
2. $H'_{\mu^*}(x^*) = -1$.
3. $\frac{\partial^2 H}{\partial \mu \partial x}(\mu^*, x^*) \neq 0$.

Then, there is an interval I *about* x^* *and a function* $p : I \to \mathbb{R}$ *such that* $H_{p(x)}(x) \neq x$ *but* $H^2_{p(x)}(x) = x$.

Details and further examples on the types of bifurcations can be found in [13],[20],[12],[35],[3].

Table 2.1: Types of bifurcation of fixed points.

Bifurcation	**Example**	$\frac{\partial H}{\partial x}(\mu^*, x^*)$	$\frac{\partial H}{\partial \mu}(\mu^*, x^*)$	$\frac{\partial^2 H}{\partial x^2}(\mu^*, x^*)$
Saddle-node	$H_\mu(x) = \mu - x^2$ $\mu^* = -\frac{1}{4}$, $x^* = -\frac{1}{2}$	1	$\neq 0$	$\neq 0$
Pitchfork	$H_\mu(x) = \mu x - x^3$ $\mu^* = 1$, $x^* = 0$	1	0	0
Transcritical	$H_\mu(x) = \mu x(1 - x)$ $\mu^* = 1$, $x^* = 0$	1	0	$\neq 0$
Period-doubling	$H_\mu(x) = \mu x(1 - x)$ $\mu^* = 3$, $x^* = \frac{2}{3}$	-1	$\neq 0$	$\neq 0$

2.5 Related Population Models

In this section, we briefly represent a variety of related biological models: some well-known single species models and the models with several interacting populations.

2.5.1 One-Dimensional Population Models

The simplest single-species model is the exponential growth model, but this model does not put a limit on the population size. Two well-known population models in which the population size is limited have been applied to a variety of populations. They are known as the Beverton-Holt model and the Ricker model. The names refer to the investigators who developed and applied these models primarily to fish populations [5],[45].

The Beverton-Holt model has the following form:

$$N_{t+1} = \frac{\lambda K N_t}{K + (\lambda - 1)N_t}, \quad \lambda > 1, K > 0.$$

The parameter $\lambda = e^r$, where r is the intrinsic growth rate. The parameter K is the carrying capacity.

The Ricker model has the following form:

$$N_{t+1} = N_t \exp\left[r\left(1 - \frac{N_t}{K}\right)\right],$$

where $r > 0$ is interpreted as intrinsic growth rate and $K > 0$ is the carrying capacity.

This model is a limiting case of the Hassell model [16] which takes the form

$$N_{t+1} = \frac{RN_n}{(1 + kN_n)^b},$$

where $R, k > 0$ and $b > 1$. When $b = 1$, the Hassel model is simply the Beverton-Holt model.

2.5.2 Two-Dimensional Population Models

2.5.2.1 Nicholson-Bailey Model

One of the most well-known model for many experimental and theoretical investigations in ecology is Nicholson-Bailey host-parasitoid model [44]. This is a discrete-time model to a biological system involved two insects, a parasitoid and its host. Nicholson and Bailey developed the model (1935) and applied it to the parasitiod (*Encarsia formosa*) and the host (*Trialeurodes vaporariorum*). The term "parasitoid" means a parasite which is free living as an adult but lays eggs in the larvae or pupae of the host. Hosts that are not parasitized give rise to their own progeny. Hosts that are successfully parasitized die but the eggs laid by the parasitoid may survive to be the next generation of parasitoids.

The general host-parasitoid model has the form

$$N_{t+1} = rN_t f(N_t, P_t), \tag{2.12}$$

$$P_{t+1} = eN_t(1 - f(N_t, P_t)), \tag{2.13}$$

where N_t is the density of host species in generation t, P_t is the density of parasitoid species in generation t, $f(N_t, P_t)$ is the fraction of hosts not parasitized, r is the number of eggs laid by a host that survive through the larvae, pupae, and adult stages, and e is the number of eggs laid by a parasitoid on a single host that survive through larvae, pupae, and adult stages. The parameter r and e are positive.

The function f can be interpreted as the probability that each individual host escapes the parasites, so that the complementary term $1 - f$ in the second equation is the probability of being parasitized. Note that if $N_t = 0$, then $P_t = 0$ that is the parasitoid cannot survive without the host. That is why parasitoids are good biological control agents.

Nicholson and Bailey model assumes a simple functional form for $f(N_t, P_t)$. f depends on the searching behavior of the parasitoid. The number encounters of the parasitoids, P_t, with the hosts, N_t is in direct proportion to host density N_t, that is, follows the law of mass action, aN_tP_t. The parameter a is the searching efficiency of the parasitoid which is the probability that a given parasitoid will encounter a given host during its searching lifetime. Since the number of encounters are distributed randomly among the available hosts, Nicholson and Bailey used the Poisson distribution: $p(n) = \frac{e^{-\mu}\mu^n}{n!}$, where n is the number of encounters and μ is the mean of encounters per host in one generation. Once the host is parasitized, it will not be parasitized again. Host with no encounters, $p(0)$, are separated from those with more than one encounter, $1 - p(0)$. The probability of encounters of the host by parasitoid represents the fraction of hosts that are not parasitized, that is, $p(0) = \frac{e^{-\mu}\mu^0}{0!} = e^{\mu}$, where $\mu = \frac{encounters}{N_t} = aP_t$, thus $p(0) = f(N_t, P_t) = \exp(-aP_t)$:

$$\begin{aligned} N_{t+1} &= rN_t \exp(-aP_t), \\ P_{t+1} &= eN_t(1 - \exp(-aP_t)). \end{aligned} \tag{2.14}$$

2.5.2.2 Beddington Model

The following density-dependent predator-prey model was investigated by Beddington et al [4]:

$$
\begin{aligned}
N_{t+1} &= N_t \exp\left[r\left(1-\frac{N_t}{K}\right) - aP_t\right], \\
P_{t+1} &= eN_t[1-\exp(-aP_t)],
\end{aligned}
\tag{2.15}
$$

where K is the carrying capacity and represents maximum population size that can be supported due to availability of all the potentially limiting resources. Note that model (2.14) reduces to the density independent one-species model $N_{t+1} = rN_t$ if the parasitoid is not present. Since this is not realistic for most of the species, model (2.15) rectifies this situation by adopting the density-depending Ricker model $N_{t+1} = N_t \exp\left[r(1-\frac{N_t}{K})\right]$, where K is the carrying capacity of the host and is the sustainable size of the host. Moreover, in the absence of the parasitiod, the equilibrium K is globally asymptotically stable for $0 < r < 2$ on $(0, \infty)$ [13]. It is assumed that the parameters a, r, e, K are all positive real numbers.

2.5.2.3 The Host-Parasitoid Model Discussed in [21]

Hone, Irle, and Thurura [21] has studied the following predator-prey system which is the more general form of the Nicholson-Bailey model, system (2.14):

$$
\begin{aligned}
N_{t+1} &= rN_t \exp(-aP_t), \\
P_{t+1} &= eN_t(1-\exp(-bP_t)).
\end{aligned}
\tag{2.16}
$$

For the special case $a = b$, the dynamics is uninteresting in the sense that either the two species can both die out, or the solutions can grow without bound. However, in general, the model displays the more biologically relevant possibilities that the two populations can asymptotically approach positive steady-state values or move towards an attracting invariant curve in the phase plane. The latter scenario arises from a Neimark-Sacker bifurcation [43], [46] that takes place in the (r, a) parameter space [21].

2.5.2.4 Generalized Beddington Model

In this thesis, we consider the following density-dependent predator-prey model which is the generalization of models (2.14), (2.15), and (2.16). In [21], the authors introduced the model as an open problem.

$$\begin{aligned} N_{t+1} &= N_t \exp\left[r\left(1 - \frac{N_t}{K}\right) - aP_t\right], \\ P_{t+1} &= eN_t[1 - \exp(-bP_t)], \end{aligned} \tag{2.17}$$

where the parameters r, K, a, b, e are positive.
Notice that in equation (2.17), when $a = b$ this is the Beddington model. With unlimited capacity, for which the term $\frac{N_t}{K}$ vanishes, equation (2.17) becomes the model discussed by Hone, *et al.* Further, if $a = b$ and the capacity is unlimited, we have Nicholson-Bailey model.

2.5.2.5 An Example of Stability Analysis of a Predator-prey Model [49]

In equation (2.12), the growth factor is rN. In Hassell's model [27], the growth factor is of the form

$$\frac{R}{(1 + kH_t)^b},$$

where $a, b > 0$ and H is the host species. Hassell et al. [27] collected R- and b-values for about two dozen species from field and laboratory observations, and noted that the majority of these cases were within the stable region.

In this section, we study the stability analysis of the following host-parasite model which is studied by Misra and Mitra [29] where the growing host is infected with the parasite:

$$\begin{aligned} H_{t+1} &= \frac{RH_t}{(1+H_t)^b} e^{-cP_t} \\ P_{t+1} &= H_t(1-e^{-cP_t}). \end{aligned} \tag{2.18}$$

Note that such simplifications, including the convention $k = 1$ in the Hassell model, lead to the interpretation of the "population" variable as a "suitable multiple of the population".

Fixed Points of System (2.18)

In order to find the fixed points (H^*, P^*) of system (2.18), we set $H_t = H_{t+1} = H^*$

and $P_t = P_{t+1} = P^*$:

$$\begin{aligned} H^* &= \frac{RH^*}{(1+H^*)^b} e^{-cP^*}, \\ P^* &= H^*(1-e^{-cP^*}). \end{aligned} \tag{2.19}$$

We first observe that for $H^* = 0$, we have the extinction fixed point $(0, 0)$ for any values of parameters. For $H^* \neq 0$ and $P^* = 0$, we obtain the solution $(R^{\frac{1}{b}} - 1, 0)$. For $H^* \neq 0$ and $P^* \neq 0$, from the first equation of the system (2.19), we have

$$P^* = \frac{1}{c} \ln \left[\frac{R}{(1+H^*)^b} \right]. \tag{2.20}$$

Now, we can see that the parameter R is important for the existence of the fixed points other than the extinction fix point (0,0). We have the following cases:

Case 1. $R \leq 1$

For this case, we have $R^{\frac{1}{b}} - 1 \leq 0$ and $\frac{1}{c} \ln \left[\frac{R}{(1+H^*)^b} \right] < 0$. Hence, there is no exclusion and coexistence fixed point for $R \leq 1$.

Case 2. $R > 1$

In the first equation of the system (2.19), assuming that $H^* \neq 0$, we have

$$e^{-cP^*} = \frac{(1+H^*)^b}{R}. \tag{2.21}$$

Combining the equation (2.21) and the second equation of the system (2.19), we obtain

$$P^* = H^* \left(1 - \frac{(1+H^*)^b}{R}\right).$$

Now, we can write the first equation of the system (2.18) as

$$H^* = \frac{RH^*}{(1+H^*)^b} e^{-cH^*\left(1-\frac{(1+H^*)^b}{R}\right)},$$

or

$$(1+H^*)^b \, e^{cH^* - \frac{c}{R}H^*(1+H^*)^b} = R, \tag{2.22}$$

an equation in the variable H^*. Let us denote

$$z = F(x) = (1+x)^b \, e^{cx - \frac{c}{R}x(1+x)^b}.$$

When the graph of F intersects the horizontal line $z = R$, some fixed points are obtained. Note that $x = R^{\frac{1}{b}} - 1$ is a solution of the equation $F(x) = R$, which corresponds to the fixed point $(R^{\frac{1}{b}} - 1, 0)$ of the system (2.18). We will investigate if there exist some other intersection points.

Setting $F'(x) = 0$, we obtain the equation

$$\frac{R(b+c+cx)}{c(1+x+bx)} = (1+x)^b.$$

For $x \geq 0$, the function on the right-hand side has y-intercept 1, and is monotonically increasing without bound. On the other hand, the function on the left-hand side is monotonically decreasing, has y-intercept $R(1+b/c) > 1$, and converges to $R/(1+b)$ as $x \to \infty$. Thus, there is a unique intersection point which means there exists only one critical point. See Figure 2.3.

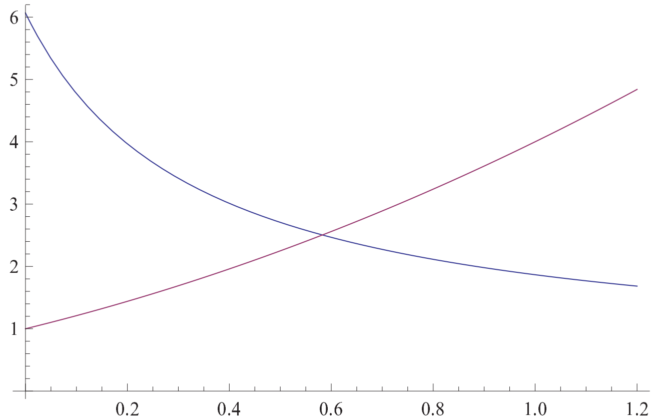

Figure 2.3: $y = \frac{R(b+c+cx)}{c(1+x+bx)}$ and $y = (1+x)^b$.
The intersection point is the point where $F'(x) = 0$.

Since $F(0) = 1$, $F'(0) = \frac{c(R-1)+bR}{R} > 0$, and $F(x) \to 0$ as $x \to \infty$, the critical point is a local maximum. See Figure 2.4.

In Figure 2.4, we know that one of the intersection points is the solution $x = R^{\frac{1}{b}} - 1$. The other intersection point, say $\bar{H}$, may or may not be a component of a positive fixed point. In order to guarantee that P component is also positive, we solve $P^* > 0$ in the equation (2.20) and obtain

$$H^* < R^{\frac{1}{b}} - 1.$$

Thus, there exists a positive fixed point if $F'(R^{\frac{1}{b}} - 1) < 0$. Solving this inequality, we obtain the condition for the existence of the positive fixed point: $R > \left(1 + \frac{1}{c}\right)^b$.

Thus, we obtain the following result.

Theorem 2.13 *For the system (2.18) the following statements hold true:*

a. If $R \leq 1$, then the only fixed point is the extinction fixed point $(0, 0)$.

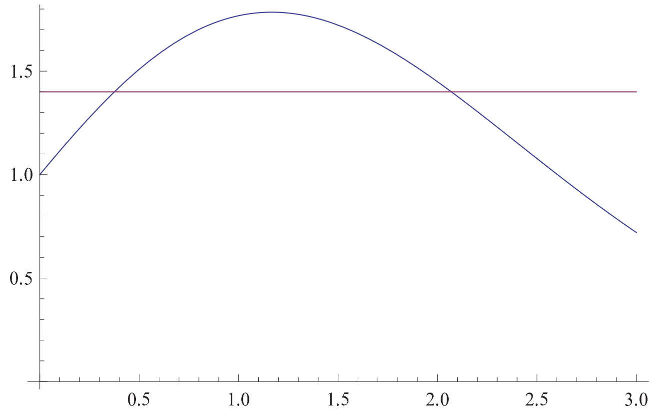

Figure 2.4: $z = F(x)$, $z = R$.
$b = 2$, $c = .6$, $R = 1.4$.

b. If

$$1 < R \leq \left(1 + \frac{1}{c}\right)^b,$$

then there exist two fixed points: the extinction fixed point $(0,0)$ *and the exclusion fixed point* $(R^{\frac{1}{b}} - 1, 0)$.

c. If

$$R > \left(1 + \frac{1}{c}\right)^b,$$

then there exist three fixed points: extinction fixed point $(0,0)$*, exclusion fixed point* $(R^{\frac{1}{b}} - 1, 0)$*, and a coexistence fixed point.*

Stability Analysis of System (2.18)

In this section, the stability of the fixed points will be examined.

The Jacobian matrix of the system (2.18) is

$$J = \begin{pmatrix} R\,(1 + H - bH)\,(1 + H)^{-1-b}\,e^{-cP} & -c\,R\,H\,(1 + H)^{-b}e^{-cP} \\ 1 - e^{-cP} & c\,H\,e^{-cP} \end{pmatrix}.$$

At $(0, 0)$, the Jacobian becomes

$$J_0 = \begin{pmatrix} R & 0 \\ 0 & 0 \end{pmatrix}.$$

The eigenvalues for the fixed point $(0, 0)$ are $\lambda_1 = R$ and $\lambda_2 = 0$. Hence, $(0, 0)$ is asymptotically stable if $R < 1$. We will now consider the exclusion fixed point.

Theorem 2.14 *For the system (2.18), the exclusion fixed point* $(R^{\frac{1}{b}} - 1, 0)$ *is asymptotically stable if*

$$\max\left(\frac{c}{c+1}, \frac{b-2}{b}\right) < R^{-\frac{1}{b}} < 1.$$

Proof. The Jacobian matrix evaluated at this point is given by

$$J_2 = \begin{pmatrix} 1 + b\left(-1 + R^{-\frac{1}{b}}\right) & -c\left(-1 + R^{\frac{1}{b}}\right) \\ 0 & c\left(-1 + R^{\frac{1}{b}}\right), \end{pmatrix}$$

where the eigenvalues are $\lambda_1 = 1 + b\left(-1 + R^{-\frac{1}{b}}\right)$ and $\lambda_2 = c\left(-1 + R^{\frac{1}{b}}\right)$. Applying the stability conditions $|\lambda_1| < 1$ and $|\lambda_2| < 1$, we obtain the desired result. □

Note that, the condition $|\lambda_2| < 1$ yields $R < \left(1 + \frac{1}{c}\right)^b$ for which there doesn't exist any coexistence fixed point. When the coexistence fixed point appears, the exclusion fixed point loses stability. We confirm our result by visual representation of the system for some values of parameters: Taking $b = 1.15$, $c = 2.2$, $R = 1.5$, for which the condition in the Theorem 2.14 is satisfied, the exclusion fixed point is locally asymptotically stable (see Figure 2.5). However, taking $c = 3.2$ and leaving the other parameters as they are, the coexistence fixed point appears and the exclusion fixed point loses stability (see Figure 2.6).

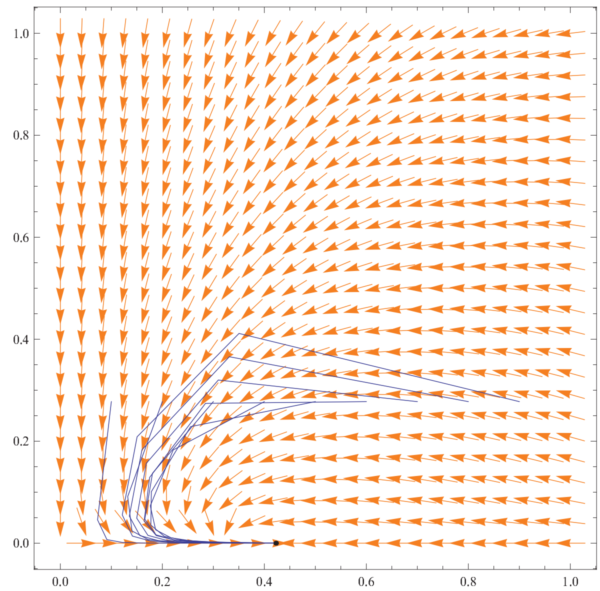

Figure 2.5: Phase portrait of system (2.18).
$b = 1.15$, $c = 2.2$, $R = 1.5$.

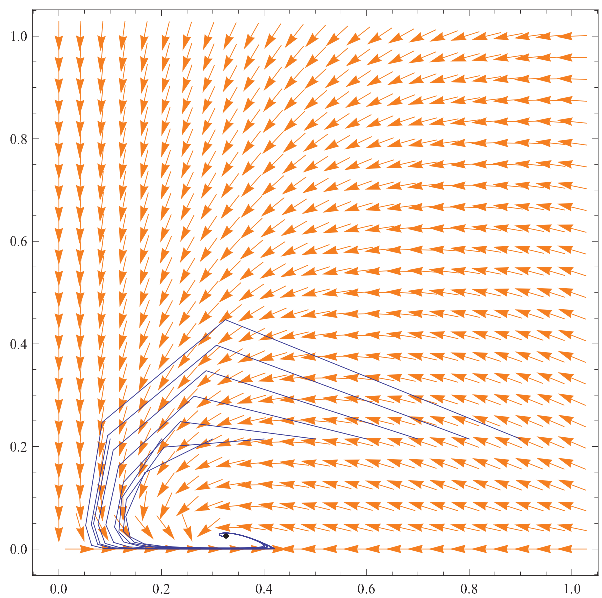

Figure 2.6: Phase portrait of the system (2.18).
$b = 1.15$, $c = 3.2$, $R = 1.5$.

Chapter 3

Population Models with Allee Effect

3.1 Allee Effect

Ecologist W.C. Allee (1931) was one of the first to write extensively on the ecological significance of animal aggregation; hence, the positive relationship between population density and the individual's fitness is often known as "Allee Effect". This effect can be caused by difficulties in, for example, mate finding, social dysfunction, inbreeding depression, food exploitation (e.g., host resistance can only be overcome by sufficient numbers of consumers), and predator avoidance or defense [1].

The most important distinction within the Allee effect domain is between component and demographic Allee effects. Component Allee effects are at the level of components of individual fitness, for example juvenile survival or litter size. Conversely, demographic Allee effects are at the level of the overall mean individual fitness, practically always viewed through the demography of the whole population as the *per capita* population growth rate [9]. The two are related in that component Allee effects may result in demographic Allee effects.

Allee proposed that the per capita birth rate declines at low population densities. Under such scenario, a population at low densities may slide into extinction. Allee found that the highest per capita growth rates of the population of the flour beetles, *Tribolium cofusum*, were at intermediate densities. Moreover, when fewer mates were available, the females produced fewer eggs, a rather unexpected outcome. Allee did not provide a definite and precise definition of this new notion. Stephens, Sutherland, and Freckleton [24] defined the Allee effect as "a positive relationship between any component of individual fitness and either numbers or density of conspecifics." In classical dynamics, we have a negative density dependence, that is, fitness decreases with increasing density. The Allee effect, however, produces a positive density dependence, that is, fitness increases with increasing density [14].

The instability of the lower equilibrium (Allee threshold) [9] means that natural populations subject to a demographic Allee effect are unlikely to persist in the range of population sizes where the effect is manifest. Another issue that may cause some confusion in the use of the term Allee effect whether the phenomenon is caused by low population sizes or by low population densities. Though for field ecologists, a drop in number will be inseparable from a corresponding reduction in density. Allee himself considered both types of Allee effect and observed the Allee effect caused by reduction in the number of mice, and the Allee effect caused by the reduction in density of our beetles, Tribolium confusum [2]. In [25], Stephens and Sutherland described several scenarios that cause the Allee effect in both animals and plants. For example, cod and many freshwater fish species have high juvenile mortality when there are fewer adults. While fewer red sea urchin give rise to worsening feeding conditions of their young and less protection from predation. In some mast flowering trees, such as *Spartina alterniflora*, with a low density have a lower probability of pollen grain finding stigma in wind-pollinated plants.

Any function f whose graph passes through the origin and remains below the diagonal near zero and later crosses the diagonal twice will give rise to the Allee effect [14].

As an example of modelling the Allee effect, consider the single-species population model

$$x_{n+1} = x_n e^{r-x_n}, \quad x_0 > 0 \tag{3.1}$$

where parameter r is positive. Model (3.1) with an Allee effect can be considered to be

$$x_{n+1} = x_n e^{r-x_n} \frac{x_n}{m+x_n}, \quad x_0 > 0. \tag{3.2}$$

The expression $\frac{x_n}{m+x_n}$ denotes the probability of an individual successfully finding a mate to reproduce or a cooperative individual to exploit resources, where parameter $m > 0$ is Allee constant [22].

3.2 A Predator-prey Model with Allee Effect

Now, we present an example of a predator-prey model with Allee effect and analyse the stability of fixed points for the model.

The following discrete-time predator-prey system was studied by Çelik and Duman [10] with an Allee effect on the prey population and by Wang, Zhang, and Liu [52] with Allee effects both on prey and predator:

$$\begin{aligned} N_{t+1} &= N_t + rN_t(1 - N_t) - aN_tP_t, \\ P_{t+1} &= P_t + aP_t(N_t - P_t), \end{aligned} \tag{3.3}$$

where the parameters a, r are positive, N_t is prey density at time t and P_t is predator density at time t, r is the intrinsic growth rate. The term aN_t is per capita predator increase due to prey consumption.

Now, we consider the system (3.3) when the predator population is subject to an Allee effect which is more general form of the system (3.1) in [52].

$$\begin{aligned} N_{t+1} &= N_t + rN_t(1 - N_t) - aN_tP_t, \\ P_{t+1} &= P_t + aP_t(N_t - P_t)\frac{P_t^d}{m + P_t^d}, \end{aligned} \tag{3.4}$$

where the parameters a, r, m are positive and $d \geq 1$.

When $d = 1$, the system is the model with Allee effect on predator discussed by Wang, Zhang, and Liu [52]. We will investigate the stability of fixed points for the model (3.4) and analyse the stability of exclusion fixed point, which is non-hyperbolic, for the particular cases when $d = 1$ and $d = 2$ by using the Center Manifold Theory.

3.2.1 Stability of Fixed Points for System (3.4)

The fixed points are $(0, 0)$, $(1, 0)$, and $(\frac{r}{a+r}, \frac{r}{a+r})$. The Jacobian matrix of the planar map in (3.4) is

$$J = \begin{pmatrix} 1 + r - 2rN - aP & -aN \\ \frac{aP^{1+d}}{m+P^d} & \frac{m^2+(1+a(N-2P))P^{2d}-mP^d(-2-a((1+d)N-(2+d)P))}{\left(m+P^d\right)^2} \end{pmatrix}.$$

The Jacobian matrix for the extinction fixed point $(0, 0)$ is

$$J_0 = \begin{pmatrix} 1 + r & 0 \\ 0 & 1 \end{pmatrix}.$$

(0,0) is unstable fixed point since one of the eigenvalues λ_1 and λ_2 is greater than 1. The Jacobian for the exclusion fixed point $(1,0)$ is

$$J_1 = \begin{pmatrix} 1-r & -a \\ 0 & 1 \end{pmatrix}.$$

Since one of the eigenvalues of the matrix J_1 is 1, this point is non-hyperbolic. By using the Center manifold theory, we will show for some particular cases, in the next section that this point is unstable.
Now, let us discuss the coexistence fixed point $(\frac{r}{a+r}, \frac{r}{a+r})$: Jacobian matrix for this point is

$$J_* = \begin{pmatrix} \frac{a+r-r^2}{a+r} & -\frac{ar}{a+r} \\ \frac{a\left(\frac{r}{a+r}\right)^{1+d}}{m+\left(\frac{r}{a+r}\right)^d} & 1-\frac{a\left(\frac{r}{a+r}\right)^{1+d}}{m+\left(\frac{r}{a+r}\right)^d} \end{pmatrix}.$$

By using the Trace-Determinant formula, after some computation we obtain the following result:

Theorem 3.1 *The positive fixed point* $(\frac{r}{a+r}, \frac{r}{a+r})$ *is asymptotically stable if*

$$0 < r[(K+m)r + a(K-Kr)] < 4a(K+m) - aKr - (K+m)(-4+r)r$$

where $K = \left(\frac{r}{a+r}\right)^d$.

In Figure 3.1, we give the numerical evidence for some particular values of the parameters that the positive fixed point is asymptotically stable.

3.2.2 Instability of Exclusion Fixed Point

In this section, by using the Center manifold theory, we show for some values of d for the system (3.4), the fixed point $(1,0)$ is unstable.

Theorem 3.2 *For the system (3.4), the following statements hold true:*

a. If $d=1$, *then* $(1,0)$ *is unstable.*

b. If $d=2$, *then* $(1,0)$ *is unstable.*

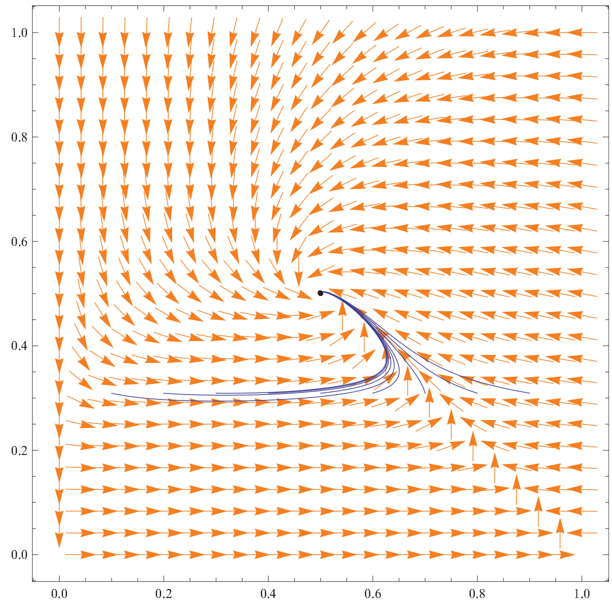

Figure 3.1: Some orbits of the system (3.4).
$m = .4,\ r = .2,\ a = .2,\ d = 2.$

Proof. The eigenvalues of the Jacobian matrix corresponding to the system given in (3.4) at the point $(1, 0)$ are $\lambda_1 = 1 - r$ and $\lambda_2 = 1$. If $r > 2$, then $|\lambda_1| > 1$ and $(1, 0)$ is unstable. Now, let us consider the case $0 < r < 2$ in which the eigenvalue $|\lambda_1| < 1$ and $\lambda_2 = 1$.

a. In order to apply the Center manifold theory, we make a change of variables in system (3.4) so we can have a shift from the point $(1, 0)$ to $(0, 0)$. Let $u = N - 1$ and $v = P$. When $d = 1$, the new system is

$$\begin{aligned} u_{t+1} &= (u_t + 1) - r(u_t + 1)u_t - a(u_t + 1)v_t - 1, \\ v_{t+1} &= v_t + av_t(u_t - v_t + 1)\frac{v_t}{m + v_t}. \end{aligned} \tag{3.5}$$

The Jacobian of the planar map given in (3.5) at the point $(0, 0)$ is

$$\tilde{J}_0 = \begin{pmatrix} 1 - r & -a \\ 0 & 1 \end{pmatrix}.$$

Now we can rewrite the equations in system (3.5) as

$$\begin{aligned} u_{t+1} &= (1-r)u_t - av_t + \tilde{f}(u_t, v_t), \\ v_{t+1} &= v_t + \tilde{g}(u_t, v_t), \end{aligned} \tag{3.6}$$

where

$$\tilde{f}(u_t, v_t) = -u_t(ru_t + av_t)$$

and

$$\tilde{g}(u_t, v_t) = \frac{a(1+u_t-v_t)v_t^2}{m+v_t}.$$

Since invariant manifold is tangent to the corresponding eigenspace by Theorem 2.9, we assume that the map h takes the form

$$h(u) = -\frac{r}{a}u + \alpha u^2 + \beta u^3 + O(u^4), \quad \alpha, \beta \in \mathbb{R}.$$

Now we can compute the constants α and β. The function h must satisfy the center manifold equation

$$h\left((1-r)u - ah(u) + \tilde{f}(u, h(u))\right) - h(u) - \tilde{g}(u, h(u)) = 0.$$

By using the Taylor series expansion we can solve the functional equation above: we obtain

$$\alpha r - \frac{r^2}{ma} = 0$$

and

$$\alpha r + \beta r + \frac{2\alpha r}{m} - \frac{r^2}{ma} - \frac{r^3}{m^2a^2} - \frac{r^3}{ma^2} - 2\alpha\left(r + a\left(\alpha - \frac{r}{a}\right)\right) = 0.$$

By solving the system we get $\alpha = \frac{r}{ma}, \beta = \frac{r^2+mr^2}{m^2a^2}$. Hence

$$h(u) = -\frac{r}{a}u + \frac{r}{ma}u^2 + \frac{r^2+mr^2}{m^2a^2}u^3.$$

Thus on the center manifold $v = h(u)$ we have the following map

$$S(u) = -\frac{u\left((1+m)r^2u^2(1+u) + ma(-m + ru(1+u))\right)}{m^2a}.$$

Since $S'(0) = 1$ and $S''(0) = -\frac{2r}{m} < 0$. Hence, in that case the exclusion fixed point $(1,0)$ is unstable.

b. Similarly, when $d = 2$, the new system is given by

$$\begin{aligned} u_{t+1} &= (u_t + 1) - r(u_t + 1)u_t - a(u_t + 1)v_t - 1, \\ v_{t+1} &= v_t + av_t(u_t - v_t + 1)\frac{v_t^2}{m + v_t^2}. \end{aligned} \tag{3.7}$$

The Jacobian of the planar map which is given in (3.7) at the point $(0,0)$ is

$$\tilde{J}_0 = \begin{pmatrix} 1-r & -a \\ 0 & 1 \end{pmatrix}.$$

Now we can write the equations in system (3.7) as

$$\begin{aligned} u_{t+1} &= (1-r)u_t - av_t + \tilde{f}(u_t, v_t), \\ v_{t+1} &= v_t + \tilde{g}(u_t, v_t), \end{aligned} \tag{3.8}$$

where

$$\tilde{f}(u_t, v_t) = -u_t(ru_t + av_t)$$

and

$$\tilde{g}(u_t, v_t) = \frac{a(1 + u_t - v_t)v_t^3}{m + v_t^2}.$$

Since invariant manifold is tangent to the corresponding eigenspace by Theorem 2.9, let us assume that the map h takes the form

$$h(u) = -\frac{r}{a}u + \alpha u^2 + \beta u^3 + O(u^4), \quad \alpha, \beta \in \mathbb{R}.$$

Now we can compute the constants α and β. The function h must satisfy the center manifold equation

$$h\Big((1-r)u - ah(u) + \tilde{f}(u, h(u))\Big) - h(u) - \tilde{g}(u, h(u)) = 0.$$

By using the Taylor series expansion we can solve the functional equation above: we obtain

$$\alpha r = 0$$

and

$$-2a\alpha^2 + (\alpha+\beta)r + \frac{r^3}{ma^2} = 0$$

By solving the system we get $\alpha = 0, \beta = -\frac{r^2}{ma^2}$. Hence

$$h(u) = -\frac{r}{a}u - \frac{r^2}{ma^2}u^3.$$

Thus on the center manifold $v = h(u)$ we have the following map

$$R(u) = \frac{mau + r^2u^3(1+u)}{ma}.$$

Since $R'(0) = 1$ and $R''(0) = 0$, we need the calculate the Schwarzian derivative [13] at the origin: The Schwarzian derivative is $\frac{6r^2}{ma} > 0$ thus the exclusion fixed point $(1,0)$ is unstable.

□

We show the influence of Allee effect on the local stability of fixed points for system (3.4). In Figure 3.2 and Figure 3.3, we show the trajectories of predator-prey densities in the system we studied. Figure 3.2 presents that the corresponding equilibrium points can move from instability to stability under Allee effect. On the other hand, Allee effect may be a destabilizing force in the predator-prey system which made the equilibrium point change from stable to unstable. Figure 3.3 presents this fact. Table 3.1 also gives a compact information about the stabilizing and destabilizing of Allee effect in the model.

Table 3.1: Allee effect may stabilize or destabilize the system.

Figure	**r**	**a**	**d**	**m**	**Fixed Point**	**Initial Point**
3.2(a), 3.2(c)	2.5	1.9	2	0	Unstable	(0.3,0.2)
3.2(b), 3.2(d)	2.5	1.9	2	0.1	Stable	(0.3,0.2)
3.3(a), 3.3(c)	2.5	0.5	2	0	Stable	(0.3,0.2)
3.3(b), 3.3(d)	2.5	0.5	2	0.3	Unstable	(0.3,0.2)

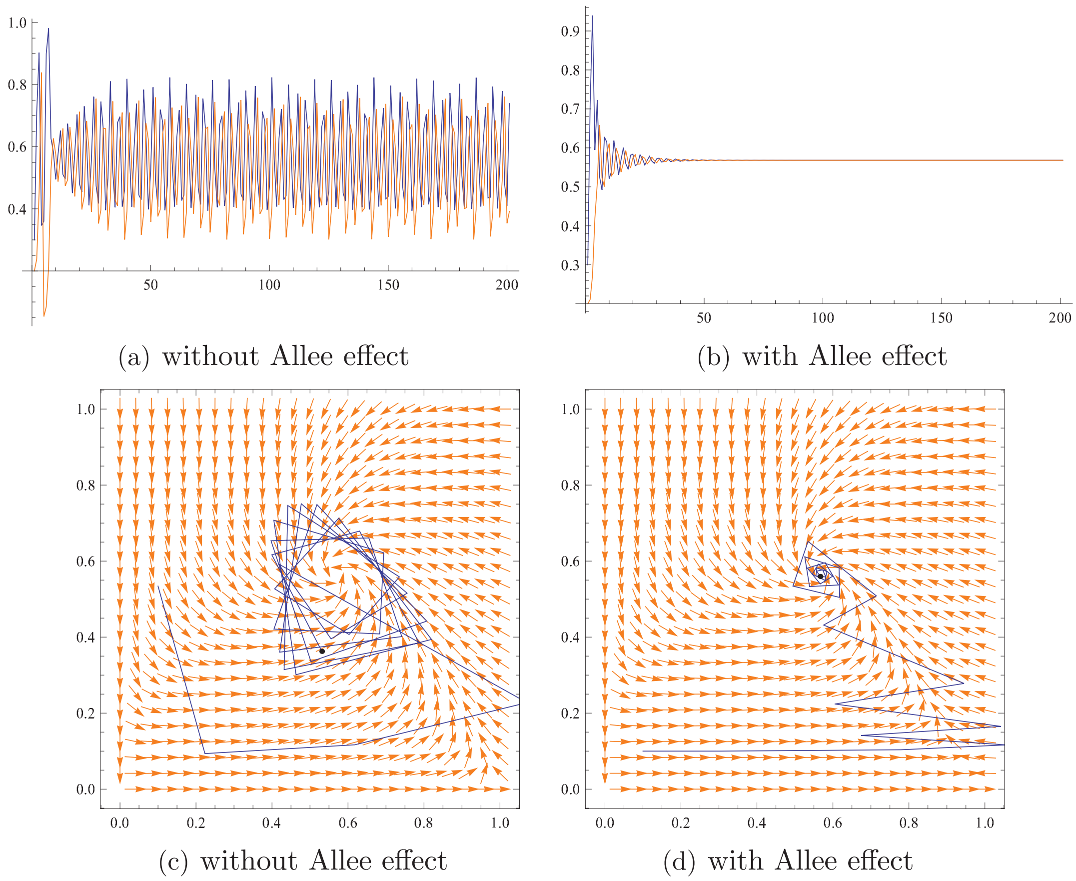

Figure 3.2: Trajectories of the prey-predator system.
Allee effect stabilizes the system. $r = 2.5$, $a = 1.9$, $d = 2$; (a),(c) $m = 0$; (b),(d) $m = 0.1$.

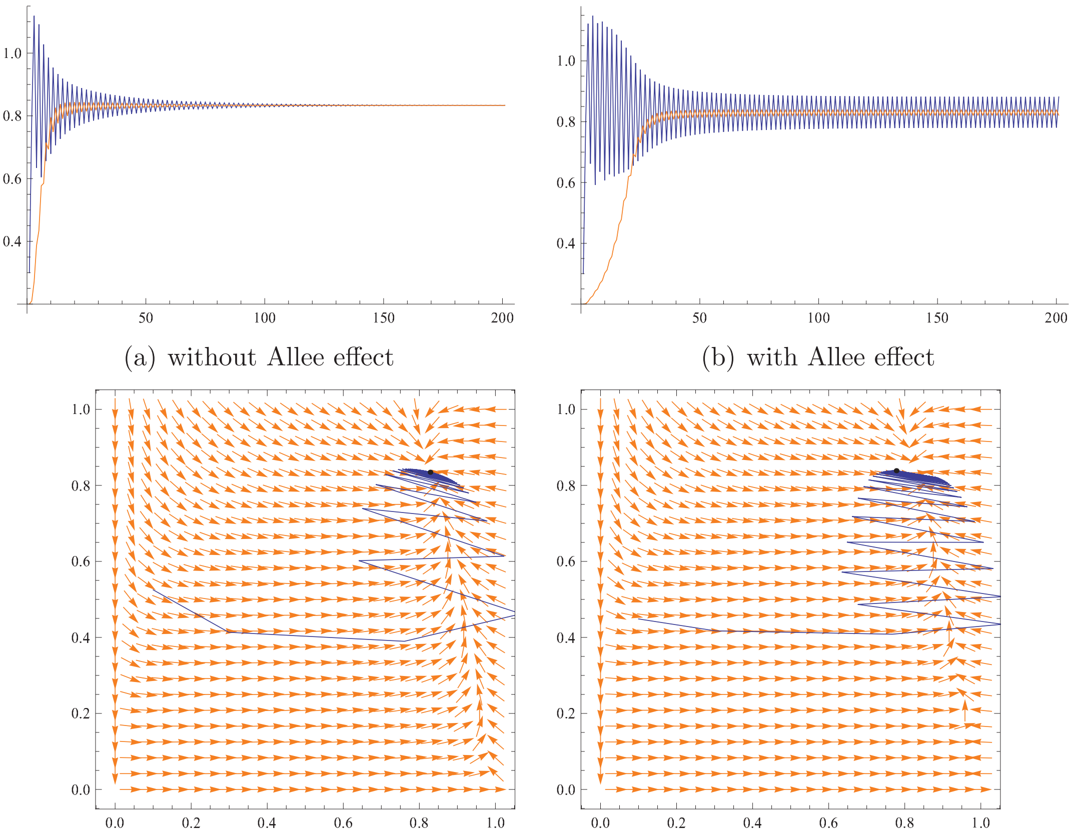

(a) without Allee effect

(b) with Allee effect

(c) without Allee effect

(d) with Allee effect

Figure 3.3: Trajectories of the prey-predator system.
Allee effect destabilizes the system. $r = 2.5$, $a = 0.5$, $d = 2$; (a),(c) $m = 0$; (b),(d) $m = 0.3$.

For more details on Allee effect, see [1],[34],[36]. Many variants of predator-prey models with Allee effect subject to predator and/or prey can be found in [9],[14],[37].

Chapter 4

Main Problem

4.1 Generalized Beddington Model

We consider the following density-dependent predator-prey model which is a generalized version of the discrete systems (2.14), (2.15), and (2.16). In [21], the authors introduced the model as an open problem.

$$\begin{aligned} N_{t+1} &= N_t \exp\left[r\left(1 - \frac{N_t}{K}\right) - aP_t\right], \\ P_{t+1} &= eN_t[1 - \exp(-bP_t)], \end{aligned} \tag{4.1}$$

where the parameters a, b, e, K, and r are positive.

Notice that in equation (4.1), when $a = b$ we obtain the Beddington model. With unlimited capacity, for which the term $\frac{N_t}{K}$ vanishes, equation (4.1) becomes the model discussed by Hone, *et al.* Further, if $a = b$ and the capacity is unlimited, we have Nicholson-Bailey model.

Now, we eliminate some of the parameters by changing the variables. Taking

$x_t = \frac{N_t}{K}$, and $y_t = bP_t$, we obtain

$$\begin{aligned} x_{t+1} &= x_t \exp\left[r\left(1 - x_t\right) - qy_t\right], \\ y_{t+1} &= \mu x_t[1 - \exp(-y_t)], \end{aligned} \tag{4.2}$$

where $\mu = beK$ and $q = \frac{a}{b}$.

All the procedures we maintain for the case $a \neq b$ in this thesis can be done for the case $a = b$ by taking $q = 1$.

4.1.1 Fixed Points

The fixed points of the discrete system (4.2) are obtained:

Theorem 4.1 *For the system given in (4.2),*

a. *if $\mu \leq 1$, then there exist two non-negative fixed points which are $(0, 0)$ and $(1, 0)$.*

b. *if $\mu > 1$, there exist three fixed points which are $(0, 0)$, $(1, 0)$ and $(\ell, \frac{r}{q}(1-\ell))$ where $0 < \ell < 1$. In this case, $(\ell, \frac{r}{q}(1-\ell))$ is coexistence (positive) fixed point.*

Proof. To find the fixed points of the system given in (4.2), the following system of equations must be solved:

$$\begin{aligned} x &= x \exp\left[r\left(1 - x\right) - qy\right], \\ y &= \mu x[1 - \exp(-y)]. \end{aligned} \tag{4.3}$$

If $x = 0$, we have the extinction fixed point $(0, 0)$ and if $x \neq 0$, the system of

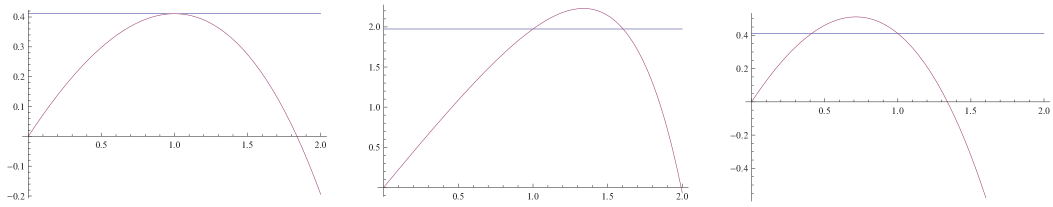

(a) $\mu = 1$ (b) $\mu < 1$ (c) $\mu > 1$

Figure 4.1: $z = F(x)$, $z = r$.

equations (4.3) becomes

$$0 = r(1 - x) - qy,$$
$$y = \mu x[1 - \exp(-y)]. \tag{4.4}$$

It is easy to find the exclusion fixed point $(1, 0)$ by taking $y = 0$ in the first equation of the system given in (4.4).

Eliminating y in (4.4), we obtain

$$r = (r + q\mu)\, x - q\mu x \exp\left[-\frac{r}{q}(1 - x)\right]. \tag{4.5}$$

Let us denote $z = F(x) = (r + q\mu)\, x - q\mu x \exp\left[-\frac{r}{q}(1 - x)\right]$. When this curve intersects the horizontal line $z = r$, some fixed points are obtained. Notice that $x = 1$ is a solution of the equation (4.5), i.e. the curves $z = F(x)$ and $z = r$ have an intersection at the point $(1, r)$ on xz-plane which corresponds to the fixed point $(1, 0)$ of the system in (4.3).

Notice that F is contiuous, $F''(x) < 0$ for all x, $\lim_{x\to\infty} F(x) = -\infty$, $F'(0) > 0$. Since $F'(1) = r(1 - \mu)$, we have the following cases:

a. If $\mu = 1$, then $F'(1) = 0$ and the only intersection point is at $x = 1$. From (4.4) we obtain $y = 0$. Hence the fixed points are $(0, 0)$ and $(1, 0)$. There are no positive fixed points for this case (See Figure 4.1(a)).

If $\mu < 1$, then $F'(1) > 0$. We know that $F''(x) < 0$ and $\lim_{x\to\infty} F(x) = -\infty$

for all x. This means that there exists another fixed point which is different from $(1,0)$. Let us denote the x-component of this fixed point by $x=\omega$, then $\omega > 1$. We have $y = \frac{r}{q}(1-\omega) < 0$ by (4.4) (See Figure 4.1(b)). Since one component of $(\omega, \frac{r}{q}(1-\omega))$ is negative, this fixed point is not of interest in biology and hence it will be omitted.

b. If $\mu > 1$, then $F'(1) < 0$. We know that $F''(x) < 0$ for all x and $F'(0) > 0$. Hence there exists another fixed point which is different from $(1,0)$. Let us denote the x-component of this fixed point by $x = \ell$. Then $\ell < 1$ and hence $y = \frac{r}{q}(1-\ell) > 0$ by (4.4) (See Figure 4.1(c)). Hence $(\ell, \frac{r}{q}(1-\ell))$ is the coexistence fixed point.

□

Lemma 4.2 *Let $f : \mathbb{R} \to \mathbb{R}$ be in C^2 where $f'(x) > 0$, $f''(x) < 0$ for all $x \in \mathbb{R}$, and let $g(x) = \alpha x + \beta$ where $\alpha, \beta \in \mathbb{R}$ and $\alpha < 0$. Furthermore, assume that $y = f(x)$ and $y = g(x)$ have an intersection point at $(\bar{x}, \bar{y})$ (Note that, there isn't another intersection point.). Take any point (x_0, y_0) on the curve $y = f(x)$ such that $x_0 > \bar{x}$.*

Then, the line tangent to the curve $y = f(x)$ at the point (x_0, y_0) intersects $g(x)$ at the point (x_1, y_1) where $\bar{y} < y_1 < y_0$.

Proof. Firstly, let us define the regions

$$R_1 = \{(x,y) : x < \bar{x}, y > \bar{y}\},$$

$$R_2 = \{(x,y) : x < \bar{x}, y < \bar{y}\},$$

$$R_3 = \{(x,y) : x > \bar{x}, y < \bar{y}\},$$

$$R_4 = \{(x,y) : x > \bar{x}, y > \bar{y}\}.$$

See Figure 4.2.

By using the monotonicity of the functions, it is easy to show that every point on the curve $y = f(x)$ lay in the set $R_2 \cup R_4 \cup \{(\bar{x}, \bar{y})\}$. Similarly, the line $y = g(x)$ lays in the set $R_1 \cup R_3 \cup \{(\bar{x}, \bar{y})\}$.

Take any point (x_0, y_0) on the curve $y = f(x)$ such that $x_0 > \bar{x}$. Since $f''(x) < 0$,

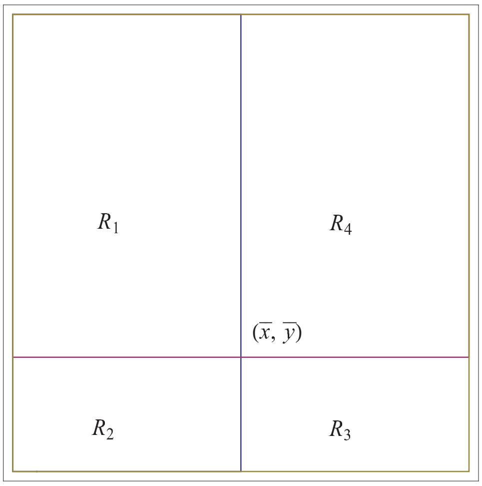

Figure 4.2: Regions R_1, R_2, R_3, R_4.

except the tangent point, every point of the tangent line at (x_0, y_0) is above the curve $y = f(x)$. The tangent line and the line $y = g(x)$ intersect at some point (x_g, y_1) since the slopes of the lines have different signs. The point (x_g, y_1) is above the function $y = f(x)$. The points on the line $y = g(x)$ which are above the curve $y = f(x)$ must be in the set R_1. Hence, the intersection occurs in that region which guaranties that $\bar{y} < y_1$. And, since the tangent line is monotonically increasing, $x_g < x_0$ implies $y_1 < y_0$. So, we have the desired result, $\bar{y} < y_1 < y_0$ (See Figure 4.3).

□

Now we construct an iteration in order to approach the intersection point of the graphs of the two functions in Lemma (4.2).

Let (x_0, y_0) be a point in the region R_4. Now, the tangent line to the curve $y = f(x)$ and passing through the point (x_0, y_0) will intersect the line $y = g(x)$ at a point, let us call it (x_{1g}, y_1). Now the horizontal line passing through the point (x_{1g}, y_1) will intersect the curve $y = f(x)$ at a point which will be denoted

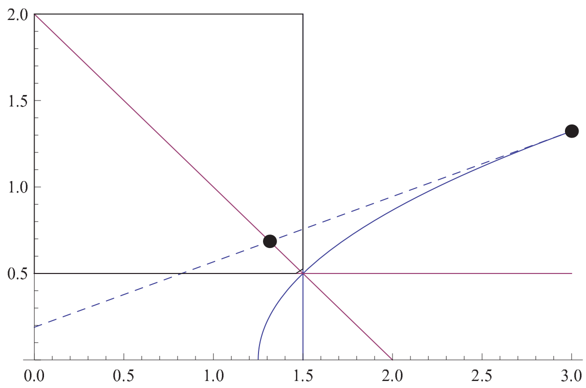

Figure 4.3: $f(x), g(x)$.

by (x_1, y_1). Next we find the point of intersection of the tangent line to $y = f(x)$ passing through the point (x_1, y_1) and the line $y = g(x)$ and we call this point (x_{2g}, y_2). Now the horizontal line through (x_{2g}, y_2) will intersect $y = f(x)$ at the point (x_2, y_2). Hence, iteratively we construct a sequence of points $\{(x_t, y_t)\}$ on the curve $y = f(x)$ in which every point (x_t, y_t) lies in the Region R_4. Consequently, we have a monotonically decreasing sequences $y_0 > y_1 > y_2 > \ldots > \bar{y}$ and $x_0 > x_1 > x_2 > \ldots > \bar{x}$. Moreover, one may show that

$$y_1 = \frac{\beta f'(x_0) - \alpha y_0 + \alpha f'(x_0) x_0}{f'(x_0) - \alpha}. \tag{4.6}$$

The next result establishes the above iteration procedure.

Theorem 4.3 *Let $f : \mathbb{R} \to \mathbb{R}$ be in C^2 where $f'(x) > 0$, $f''(x) < 0$ for all $x \in \mathbb{R}$. Consider $g(x) = \alpha x + \beta$ where $\alpha, \beta \in \mathbb{R}$ and $\alpha < 0$. Furthermore, assume that f and g intersect at the point $(\bar{x}, \bar{y})$. If $x_0 > \bar{x}$, then for any initial value $y_0 = f(x_0)$, $\bar{y}$ is the only fixed point of the difference equation*

$$Y_{t+1} = \frac{\beta + \alpha u(Y_t) - \alpha Y_t u'(Y_t)}{1 - \alpha u'(Y_t)},$$

where $u = f^{-1}$. Moreover, this fixed point is asymptotically stable.

Proof. In order to find the fixed points we solve the following equation:

$$Y = \frac{\beta + \alpha u(Y) - \alpha Y u'(Y)}{1 - \alpha u'(Y)}.$$

Hence, we obtain

$$Y = \alpha f^{-1}(Y) + \beta. \tag{4.7}$$

It is clear that $\bar{y}$ is a solution. Since the function f is increasing ($f'(x) > 0$), so is f^{-1}. Hence, by the fact that the function at the left-hand side of equation (4.7) is increasing and the one on the right-hand side is decreasing, there can be only one solution. We conclude that $Y = \bar{y}$ is the only solution.

By Lemma 4.2, Y_t is decreasing and bounded below. Hence, its limit is the fixed point $Y = \bar{y}$. □

Now, we are ready to focus on the isoclines of system (4.2):

$$\begin{aligned} y &= -\frac{r}{q}x + \frac{r}{q}, \\ y &= \mu x \left(1 - e^{-y}\right). \end{aligned} \tag{4.8}$$

By Theorem 4.3 we have

$$\begin{aligned} g(x) &= -\frac{r}{q}x + \frac{r}{q}, \\ x = f^{-1}(y) &= \frac{y}{\mu \left(1 - e^{-y}\right)}. \end{aligned} \tag{4.9}$$

By Lemma 4.1, if $\mu > 1$ we have a positive fixed point which means that the isoclines have a point of intersection. We have $\alpha = -\frac{r}{q} < 0$ and $\beta = \frac{r}{q}$. Moreover, $f'(x) > 0$ and $f''(x) < 0$. Hence, by Theorem 4.3, the difference equation that have $\bar{y}$ as its fixed point is given by

$$y_{t+1} = \frac{r\left(\mu + e^{2y_t}\mu - e^{y_t}\left(y_t^2 + 2\mu\right)\right)}{q\mu + e^{2y_t}(r + q\mu) - e^{y_t}(r + ry_t + 2q\mu)} = G(y_t). \tag{4.10}$$

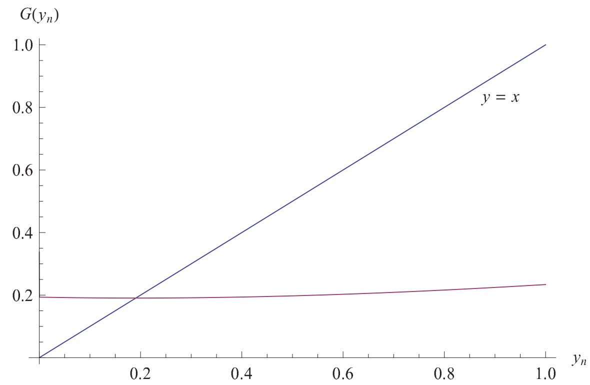

Figure 4.4: $y_{t+1} = G(y_t)$.
$\mu = 2.1$, $r = 2.7$, $q = 1.2$.

The graph of the function $y_{t+1} = G(y_t)$, in equation (4.10), is given in Figure 4.4 for some particular values of parameters.

The iteration is shown in Figure 4.5.

The iteration in equation (4.10) gives rise to the sequence $\{(X_t, Y_t)\}$ with $Y_t > y^*$. We now create a new sequence $\{(X_t, \tilde{Y}_t)\}$, where $\tilde{Y}_t$ is the y-component of the point on the isocline $y = \frac{r}{q}(1-x)$ with the x-component equals to X_t.

Now $X_t = f(Y_t) = \frac{Y_t}{\mu(1-e^{-Y_t})}$. Hence, the equation for $\tilde{Y}_t$ is given by

$$\tilde{Y}_t = \frac{r}{q}\left(1 - \frac{Y_t}{\mu(1-e^{-Y_t})}\right).$$

So for $Y_0 > y^*$, we have

$$\tilde{Y}_t < y^* < Y_t \quad \text{for all} \quad t \geq 0. \tag{4.11}$$

We will use this fact in studying the stability of the coexistence fixed point (x^*, y^*).

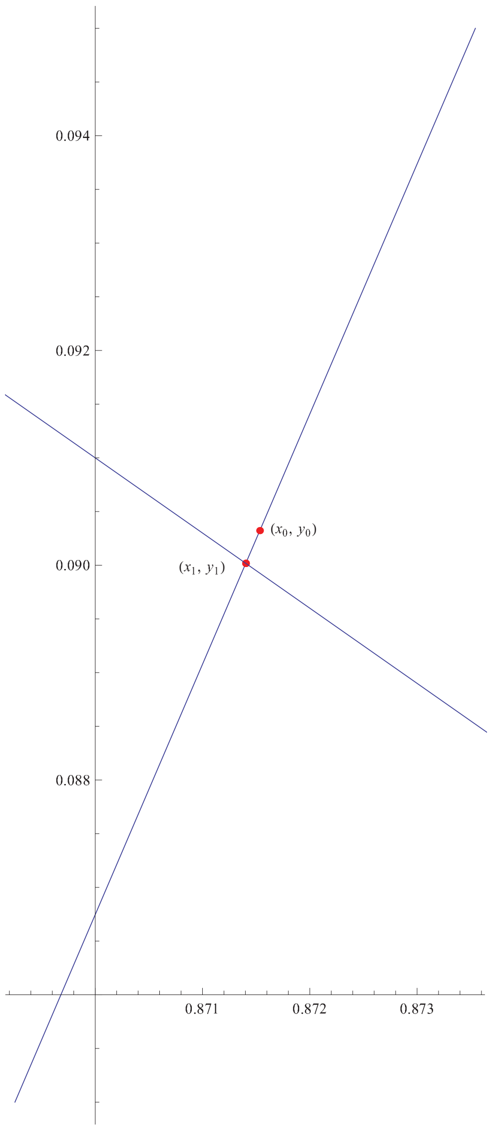

Figure 4.5: Isoclines and the iterations of $y_t = G(y_t)$.

4.1.2 Stability of Fixed Points for system (4.2)

4.1.2.1 Stability of extinction and exclusion fixed points

Theorem 4.4 *For system (4.2), the following statements hold true:*

a. $(0,0)$ *is unstable.*

b. $(1,0)$ *is asymptotically stable if* $0 < \mu < 1$ *and* $0 < r \leq 2$ *or* $0 < \mu \leq 1$ *and* $0 < r < 2$.

Proof. The Jacobian matrix of the map

$$G(x,y) = \left(x \exp\left[r\left(1-x\right) - qy\right], \mu x[1 - \exp(-y)]\right)$$

is

$$JG(x,y) = \begin{pmatrix} e^{r-rx-qy}(1-rx) & -qe^{r-rx-qy}x \\ \mu - e^{-y}\mu & e^{-y}\mu x \end{pmatrix}.$$

a. The Jacobian evaluated at the point $(0,0)$ is

$$JG(0,0) = \begin{pmatrix} e^r & 0 \\ 0 & 0 \end{pmatrix}.$$

The eigenvalues of $JG(0,0)$ are 0 and e^r. Since $r > 0$, $e^r > 1$. Thus $(0,0)$ is unstable. We also notice that any point with the form $(0,y)$ is eventually fixed point, because starting with $(0,y)$, we get $G(0,y) = (0,0)$.

b. The Jacobian evaluated at $(1,0)$ is

$$JG(1,0) = \begin{pmatrix} 1-r & -q \\ 0 & \mu \end{pmatrix}.$$

The eigenvalues for this matrix are $\lambda_1 = 1 - r$ and $\lambda_2 = \mu$. Thus $\rho(JG(1,0)) < 1$ if and only if $0 < r < 2$ and $0 < \mu < 1$. Hence $(1,0)$ is locally asymptotically stable if $0 < r < 2$ and $0 < \mu < 1$.

Two issues remain unresolved. The first is the case when $\mu = 1$ and $r < 2$ in which the eigenvalue $|\lambda_1| < 1$ and $\lambda_2 = 1$. The second case is when $\mu < 1$ and $r = 2$ in which the eigenvalue $\lambda_1 = -1$ and $|\lambda_2| < 1$.

Let us now consider the first case. In order to apply the center manifold theorem [13], it is more convenient to make a change of variables in system (4.2) so we can have a shift from the point $(1,0)$ to $(0,0)$. Let $u = x - 1$ and $v = y$. Then the new system is given by

$$\begin{aligned} u_{t+1} &= (u_t + 1)\exp\left[-ru_t - qv_t\right] - 1, \\ v_{t+1} &= \mu(u_t + 1)[1 - \exp(-v_t)]. \end{aligned} \tag{4.12}$$

The Jacobian of the planar map given in (4.12) is

$$\tilde{J}G(u,v) = \begin{pmatrix} -e^{-ru-qv}(-1 + r + ru) & -e^{-ru-qv}q(1+u) \\ \mu - e^{-v}\mu & e^{-v}(1+u)\mu \end{pmatrix}.$$

At $(0,0)$, $\tilde{J}G$ has the form

$$\tilde{J}G(0,0) = \begin{pmatrix} 1-r & -q \\ 0 & \mu \end{pmatrix}.$$

When $\mu = 1$, we have

$$\tilde{J}G(0,0) = \begin{pmatrix} 1-r & -q \\ 0 & 1 \end{pmatrix}.$$

Now we can write the equations in system (4.12) as

$$\begin{aligned} u_{t+1} &= (1-r)u_t - qv_t + \tilde{f}(u_t, v_t), \\ v_{t+1} &= v_t + \tilde{g}(u_t, v_t), \end{aligned} \tag{4.13}$$

where

$$\tilde{f}(u_t, v_t) = -1 + (-1+r)u_t + e^{-ru_t - qv_t}(1+u_t) + qv_t$$

and

$$\tilde{g}(u_t, v_t) = \mu(1+u_t) - \mu e^{-v_t}(1+u_t) - v_t.$$

Since invariant manifold is tangent to the corresponding eigenspace by Theorem 2.9, let us assume that the map h takes the form

$$h(v) = -\frac{q}{r}v + \alpha v^2 + \beta v^3 + O(v^4), \quad \alpha, \beta \in \mathbb{R}.$$

Now we are going to compute the constants α and β. The function h must satisfy the center manifold equation

$$h(v + \tilde{g}(h(v), v)) - \Big[(1-r)h(v) + qv - \tilde{f}(h(v), v)\Big] = 0.$$

The Taylor series expansions, at the point $v = 0$, are evaluated for the equation above. Equating the coefficients of the series, we obtain the system of equations

$$\frac{q^2}{r^2} + \frac{q}{2r} + \alpha r = 0$$

and

$$3q^2 + 6r^2(\alpha - \beta r) + qr\left(1 + 6\alpha(3+r)\right) = 0.$$

Solving the system we get

$$\alpha = -\frac{q(2q+r)}{2r^3},$$

$$\beta = \frac{q\left(-15qr + (-3+r)r^2 - 6q^2(3+r)\right)}{6r^5}.$$

Thus on the center manifold $u = h(v)$ we have the following map

$$P(v) = \frac{1}{6}\left(6 - \frac{6qv}{r} - \frac{3q(2q+r)v^2}{r^3} + \frac{q\left(-15qr + (-3+r)r^2 - 6q^2(3+r)\right)v^3}{r^5}\right) \times \left(1 - e^{-v}\right).$$

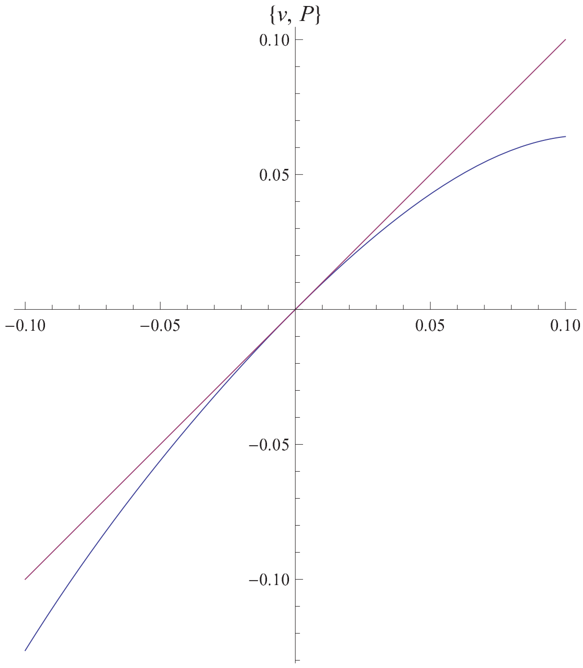

Figure 4.6: The map P on the center manifold $u = h(v)$
$\mu = 1$, $q = 1.6$ and $r = .8$.

Calculations show that $P'(0) = 1$ and $P''(0) = -1 - \frac{2q}{r} < 0$. Hence, for the map P, the origin is semistable from the right. See Figure 4.6.

The numerical evidence that $u = h(v)$ is a good candidate for a center manifold is shown in Figure 4.7.

Thus, for this case the exclusion fixed point is asymptotically stable.

Now, let us consider the case that $\mu < 1$ and $r = 2$ in which the eigenvalue $\lambda_1 = -1$ and $|\lambda_2| < 1$.

When $r = 2$ we have

$$\tilde{J}G(0,0) = \begin{pmatrix} -1 & -q \\ 0 & \mu \end{pmatrix}.$$

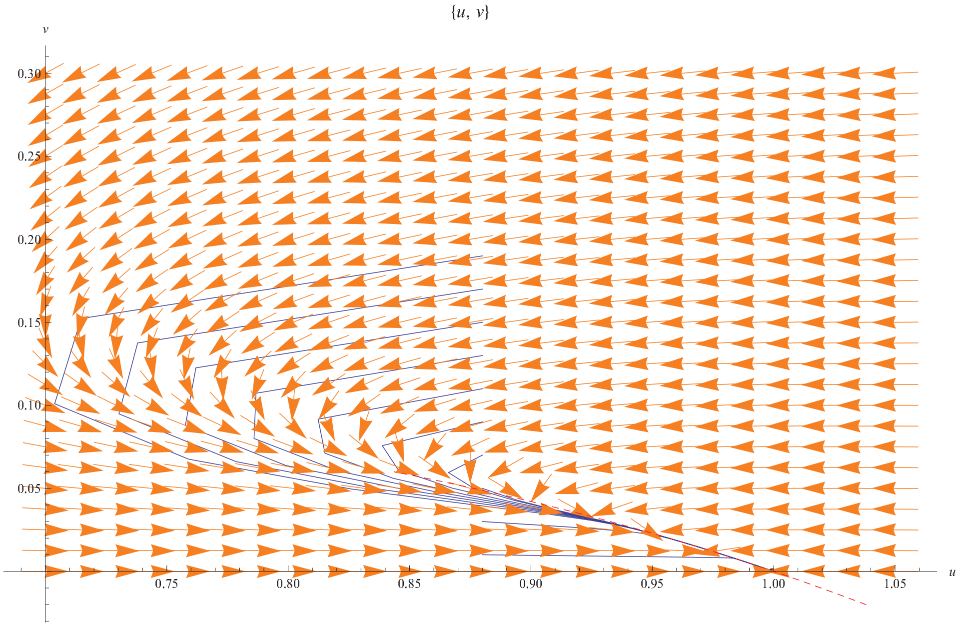

Figure 4.7: The center manifold $u = h(v)$.
(the dashed curve) $\mu = 1$, $q = 1.6$, and $r = .8$.

Now we can write the equations in system (4.12) as

$$\begin{aligned} u_{t+1} &= -u_t - qv_t + \tilde{f}(u_t, v_t), \\ v_{t+1} &= \mu v_t + \tilde{g}(u_t, v_t), \end{aligned} \tag{4.14}$$

where

$$\tilde{f}(u_t, v_t) = -1 + u_t + e^{-2u_t - qv_t}(1 + u_t) + qv_t$$

and

$$\tilde{g}(u_t, v_t) = (1 - e^{-v_t})\mu(1 + u_t) - \mu v_t.$$

By Theorem 2.9, let us assume that the map h takes the form

$$h(u) = \alpha u^2 + \beta u^3 + O(u^4), \quad \alpha, \beta \in \mathbb{R}.$$

Now we are going to compute the constants α and β. The function h must satisfy the center manifold equation

$$h(-u - qh(u) + \tilde{f}(u, h(u))) - \mu h(u) - \tilde{g}(u, h(u)) = 0.$$

Solving the above functional equation yields:

$$\alpha - \alpha\mu = 0$$

and

$$2\alpha^2 q - \alpha\mu - \beta(1+\mu) = 0.$$

Hence, $\alpha = \beta = 0$. Hence $h(u) = 0$. Thus on the center manifold $v = 0$ we have the following map

$$Q(u) = -1 + e^{-2u}(1+u).$$

Simple calculations show that $Q'(0) = -1$. The Schwarzian derivative of the map Q at the origin is $-4 < 0$. Hence, the exclusion fixed point $(1, 0)$ is asymptotically stable.

□

4.1.2.2 The estimation of the stability region of the coexistence fixed point in the parameter space

In this section, the estimation of the stability region of the coexistence fixed point in r-μ parameter space is presented.

Lemma 4.5 *For the functions $f, g, \tilde{f}, \tilde{g} : \mathbb{R}^2 \to \mathbb{R}$, let*

$$A = \{(a,b) : f(a,b) < g(a,b)\},$$

$$\tilde{A} = \{(a,b) : \tilde{f}(a,b) < \tilde{g}(a,b)\}.$$

If $f(a,b) < \tilde{f}(a,b)$ and $\tilde{g}(a,b) < g(a,b)$ for all $a, b \in \mathbb{R}$, then $\tilde{A} \subset A$.

Proof. For $\tilde{A} = \emptyset$, it is trivial. Now let $\tilde{A} \neq \emptyset$. Take $(x_0, y_0) \in \tilde{A}$. Then $\tilde{f}(x_0, y_0) < \tilde{g}(x_0, y_0)$. Hence, $f(x_0, y_0) < \tilde{f}(x_0, y_0) < \tilde{g}(x_0, y_0) < g(x_0, y_0)$ from which we conclude that $(x_0, y_0) \in A$. Thus, $\tilde{A} \subset A$. □

In Section 4.1.1, we give a symbolic approximation of the coexistence fixed point. To obtain the stability region for the fixed point, we use equation (4.11), Lemma 4.5 and the following Trace-Determinant Formula:

$$|Tr(J^*)| - 1 < Det(J^*) < 1,$$

where J^* is the Jacobian matrix evaluated at the coexistence fixed point.

It is equivalent to

$$Det(J^*) < 1 \wedge Det(J^*) > Tr(J^*) - 1 \wedge Det(J^*) > -Tr(J^*) - 1.$$

Firstly, we convert the Jacobian of the system at the coexistence fixed point (x^*, y^*) to the following form in which, x^* is eliminated:

$$J^* = \begin{pmatrix} 1 - r + qy^* & -q + \frac{q^2 y^*}{r} \\ \frac{ry^*}{r - qy^*} & \mu - y^* - \frac{\mu q y^*}{r} \end{pmatrix}.$$

The determinant and the trace of J^* are:

$$Det\,(J^*) = \frac{1}{r}\left[r^2(y^* - \mu) - qy^*(1 + qy^*)\mu + r\left(-qy^{*2} + \mu + y^*(-1 + q + 2q\mu)\right)\right],$$

$$Tr\,(J^*) = 1 - r + (-1 + q)y^* + \mu - \frac{qy^*\mu}{r}.$$

Case 1. $Det(J^*) < 1$

The region on r-μ parameter space for the condition $Det(J^*) < 1$ is given by

$$A = \{(r, \mu) : \mu r - \mu r^2 - r + (2\mu r q + r^2 + qr)y^* < (qr + q^2\mu)y^{*2} + (r + q\mu)y^*\}.$$

Let

$$A_t = \{(r, \mu) : \mu r - \mu r^2 - r + (2\mu r q + r^2 + qr)Y_t < (qr + q^2\mu)\tilde{Y}_t^2 + (r + q\mu)\tilde{Y}_t\}. \quad (4.15)$$

By Lemma 4.5 and the bounds in equation (4.11), we have $A_t \subset A$ for all $t \geq 0$. Similarly, we obtain $A_0 \subset A_1 \subset A_2 \subset \cdots \subset A_t \subset \cdots \subset A$. Hence, for every point (r, μ) in the region A_t, the condition $Det(J^*) < 1$ is satisfied for any t.

Case 2. $Tr(J^*) < 1 + Det(J^*)$

By using the similar idea as Case 1, we convert this inequality to the form where both sides are monotonic functions with respect to y^* and use the bounds in equation (4.11) to obtain the region

$$B_t = \{(r, \mu) : r^2 - \mu r^2 + (2\mu qr + r^2)\tilde{Y}_t > (\mu q^2 + qr)Y_t^2\}. \tag{4.16}$$

Case 3. $-1 - Det(J^*) < Tr(J^*)$

For this case, similarly we obtain the region

$$\begin{aligned} C_t = \{(r, \mu) : -2r - 2\mu r + r^2 + \mu r^2 + (2\mu q + 2r)Y_t + (mq^2 + qr)Y_t^2 < \\ \left(2mqr + r^2 + 2qr\right)\tilde{Y}_t\}. \end{aligned} \tag{4.17}$$

In order to obtain the stability region in the (r, μ) plane, let us take $q = 1.6$. By numeric computations, we obtain the regions A_5, B_5, and C_5 which are subsets of the regions satisfying $Det(J^*) < 1$, $Det(J^*) > Tr(J^*) - 1$ and $Det(J^*) > -Tr(J^*) - 1$, respectively. Since the intersection of the sets A_5, B_5, and C_5 is a subset of the stability region, finally, we obtain the approximated stability region of the coexistence fixed point. Furthermore, on the borderline of the stability region, we have Neimark-Sacker bifurcation when $Det(J^*) = 1$; saddle-node bifurcation when $Det(J^*) = Tr(J^*) - 1$ and period-doubling bifurcation when $Det(J^*) = -Tr(J^*) - 1$. In Figure 4.8, the approximated stability region and the types of bifurcation appearing on the borderline of the region is presented.

The approximated stability region for some particular values of parameter q

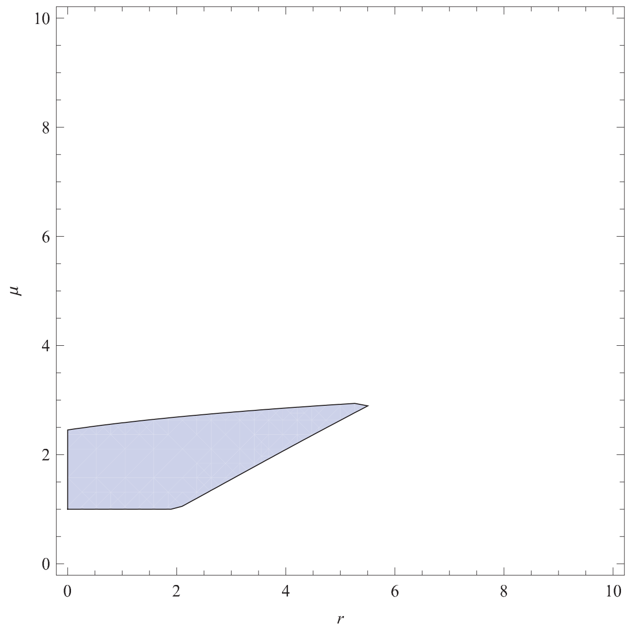

Figure 4.8: $A_5 \cap B_5 \cap C_5$.
Approximated stability region for coexistence fixed point, where $q = 1.6$.

is given in Figure 4.9. Note that, when $q = 1$, which is the case $a = b$, is the region given in [11].

4.1.3 Stable and Unstable Manifolds

For the point $(0, 0)$, since $|\lambda_1| = e^r > 1$ and $|\lambda_2| = 0 < 1$, the extinction fixed point is a saddle for all values of the parameters r and μ. For this point, the x axis is the unstable manifold and the y axis is the stable manifold.
Now, let us focus on the exclusion fixed point, $(1, 0)$: By using a similar procedure to that used for the center manifold in the proof of Lemma 4.4, we obtain the stable and unstable manifolds. In model (4.2), the saddle scenario for the exclusion fixed point occurs when $r > 2$, $\mu < 1$ or $r < 2$, $\mu > 1$.

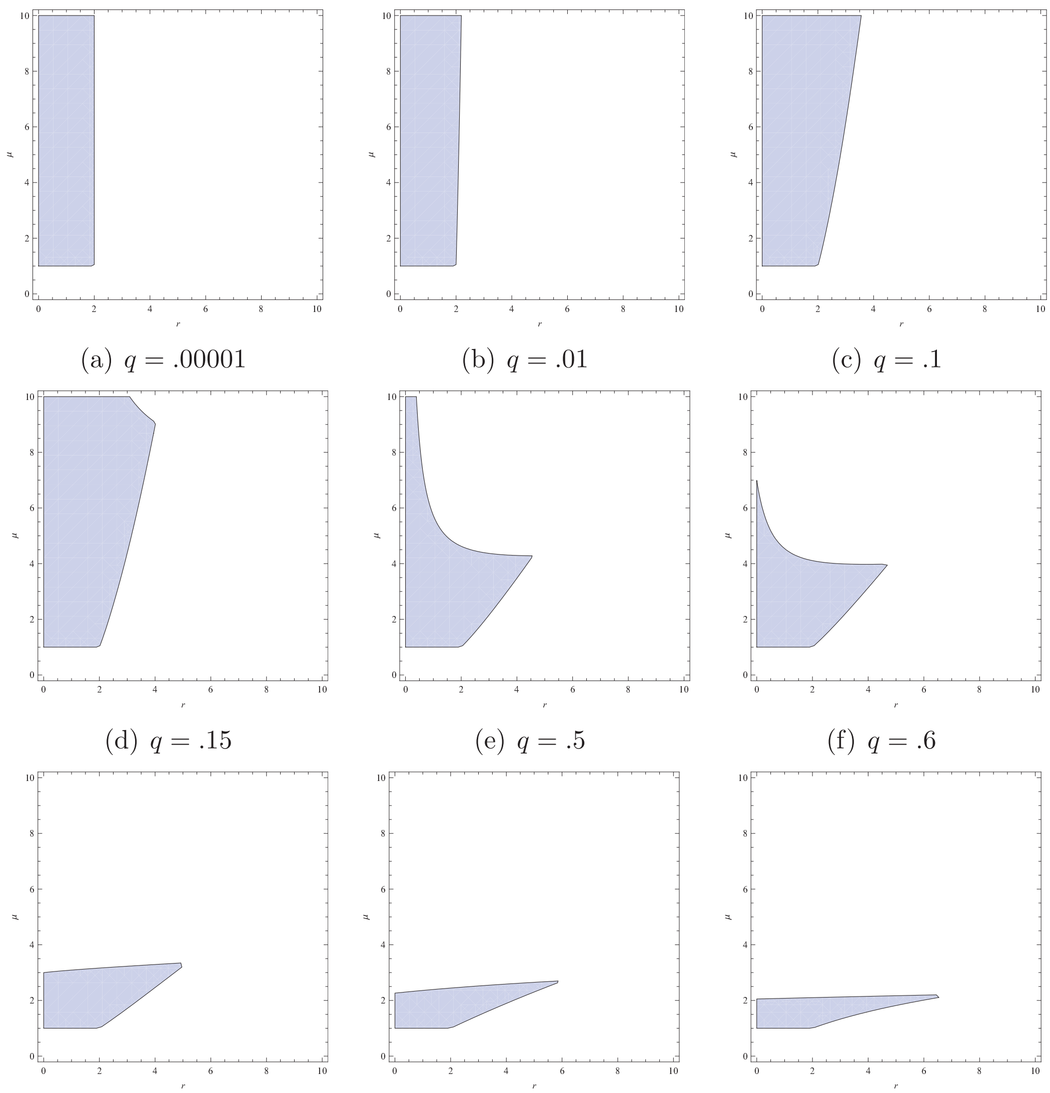

(a) $q = .00001$ (b) $q = .01$ (c) $q = .1$

(d) $q = .15$ (e) $q = .5$ (f) $q = .6$

(g) $q = 1$ (h) $q = 2.4$ (i) $q = 10$

Figure 4.9: Approximated stability region for coexistence fixed point.

Case 1. $r > 2$ **and** $\mu < 1$

Shifting the exclusion fixed point from $(1, 0)$ to $(0, 0)$ we have the following Jacobian matrix:

$$\tilde{J}G(0,0) = \begin{pmatrix} 1-r & -q \\ 0 & \mu \end{pmatrix}.$$

Now we can write the equations in system (4.12) as

$$\begin{aligned} u_{t+1} &= (1-r)u_t - qv_t + \tilde{f}(u_t, v_t), \\ v_{t+1} &= \mu v_t + \tilde{g}(u_t, v_t), \end{aligned} \tag{4.18}$$

where

$$\tilde{f}(u_t, v_t) = -1 + (-1+r)u + e^{-ru-qv}(1+u) + qv$$

and

$$\tilde{g}(u_t, v_t) = \left(1 - e^{-v}\right)\mu(1+u) - \mu v.$$

Notice that since $\mu < 1$, by Theorem 2.9 the stable manifold is tangent to the corresponding eigenspace at the fixed point. Hence, we assume that the map h takes the form

$$h(v) = \frac{q}{1-\mu-r}v + \alpha v^2 + \beta v^3 + O(v^4), \quad \alpha, \beta \in \mathbb{R}.$$

The function h must satisfy the equation

$$h\left(\mu v + \tilde{g}(h(v), v)\right) - (1-r)h(v) + qv - \tilde{f}(h(v), v) = 0.$$

In order to solve the functional equation, the Taylor series expansions of required functions are calculated and solving the system we get α and β which locally determine the stable manifold $u = h(v)$ for the exclusion fixed points. Due to the big size of the formulas for the constants α and β we omit them. In Figure 4.10, the stable manifold is presented. There are two orbits with initial

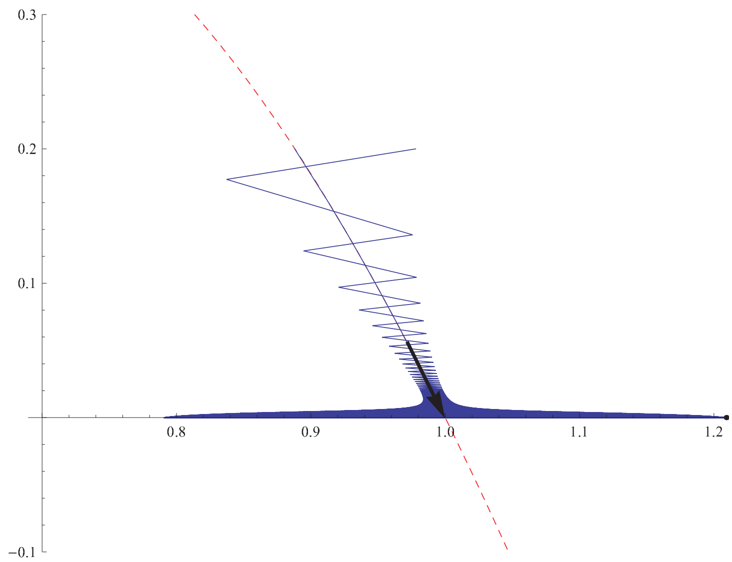

Figure 4.10: Stable manifold for the fixed point $(1, 0)$ (the dashed curve). $r = 2.03 > 2$, $\mu = .9 < 1$, $q = 1.2$.

points $(.888, .2)$ and $(.98, .2)$. The first initial point is almost on the stable manifold.

In order to find the unstable manifold for the exclusion fixed point, we use the same idea. However, we assume here that the map h takes the form

$$h(u) = \alpha u^2 + \beta u^3 + O(u^4), \quad \alpha, \beta \in \mathbb{R}.$$

We obtain that $\alpha = 0$ and $\beta = 0$.

When $y_t = 0$ in the equation (4.2), the dynamics of population x_t is determined by the one-dimensional Ricker map. If $2 < r < r_2$, where $r_2 \approx 2.5264$, the fixed point $(1, 0)$ loses its stability and a new asymptotically periodic orbit $\{\bar{x}_1, \bar{x}_2\}$ of period 2 is born. The unstable manifold is the open interval $(\bar{x}_1, \bar{x}_2)$ that lies on the x-axis. As r increases, period-doubling bifurcation occurs until $r \approx 2.6294$, after which we enter the chaotic region. Hence the boundary of the unstable manifold shrinks to 0 as $r > 2$ increases. More details on the periodic points of the Ricker map and the basin of attractions of its periodic orbits may be found in [15].

Case 2. $r < 2$ **and** $\mu > 1$

In order to find the unstable manifold for this case; since invariant manifold is tangent to the corresponding eigenspace by Theorem 2.9, let us assume that the map h takes the form

$$h(v) = \frac{q}{1-\mu-r}v + \alpha v^2 + \beta v^3 + O(v^4), \quad \alpha, \beta \in \mathbb{R}.$$

Since $\mu > 1$, the unstable manifold is tangent to the corresponding eigenvector at the fixed point.

Since the method we use for this case is the same as in the previous case, we omit the details.
In order to find the stable manifold for the exclusion fixed point, we assume that the map h takes the form

$$h(u) = \alpha u^2 + \beta u^3 + O(u^4), \quad \alpha, \beta \in \mathbb{R}.$$

See Figure 4.11.

4.1.4 Bifurcation Scenarios

In this section, a bifurcation diagram for the positive fixed point is presented. In Figure 4.13, Tr-Det Diagram for a general system is shown. We give the corresponding regions for system (4.2) in Figure 4.14: B_i is the corresponding region for A_i.

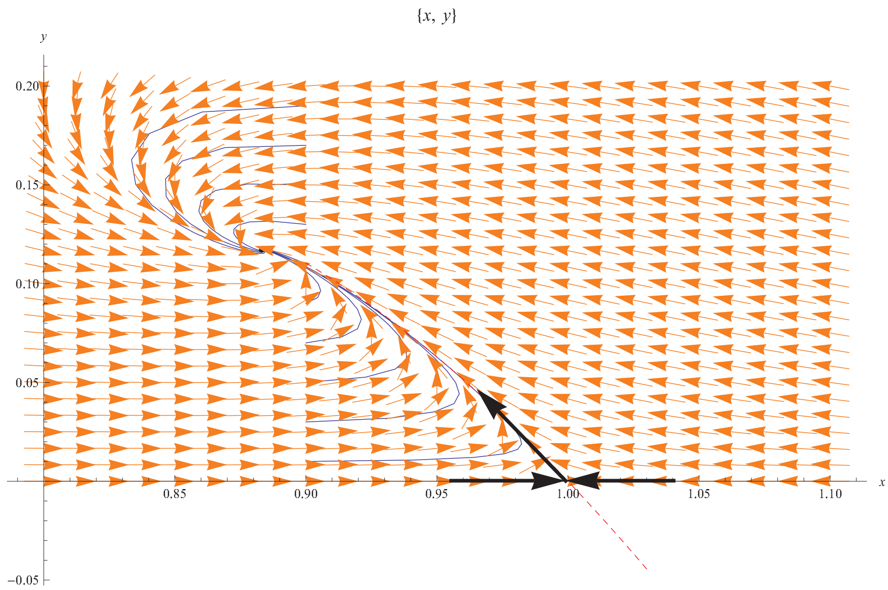

Figure 4.11: Stable and unstable manifolds for the fixed point $(1, 0)$. $\mu = 1.2 > 1$, $r = .5 < 2$, and $q = .5$.

We can see from these figures that on the border between the stability region and region B_3, we have period-doubling bifurcation. The saddle-node bifurcation occurs when the point (r, μ) moves from the stability region to region B_7. We find that the map $u = P(v)$ obtained by the center manifold theorem satisfies the conditions $\frac{\partial P}{\partial \mu}(0, 1) = 0$ and $\frac{\partial^2 P}{\partial \mu^2}(0, 1) = 0$. Hence, this bifurcation is a transcritical bifurcation [13].

The system also possesses a Neimark-Sacker bifurcation when the parameters are on the border between the stability region and region B_1 as shown in Figure 4.12.

Figure 4.15 depicts the phase-space diagram and regions in the parameter space when (r, μ) is in the stability region and close to the border of the Neimark-Sacker bifurcation. The case when the point (r, μ) passes the bifurcation curve is given in Figure 4.16. The black points in Figure 4.15 (a) and Figure 4.16 (a) represent the point (r, μ).

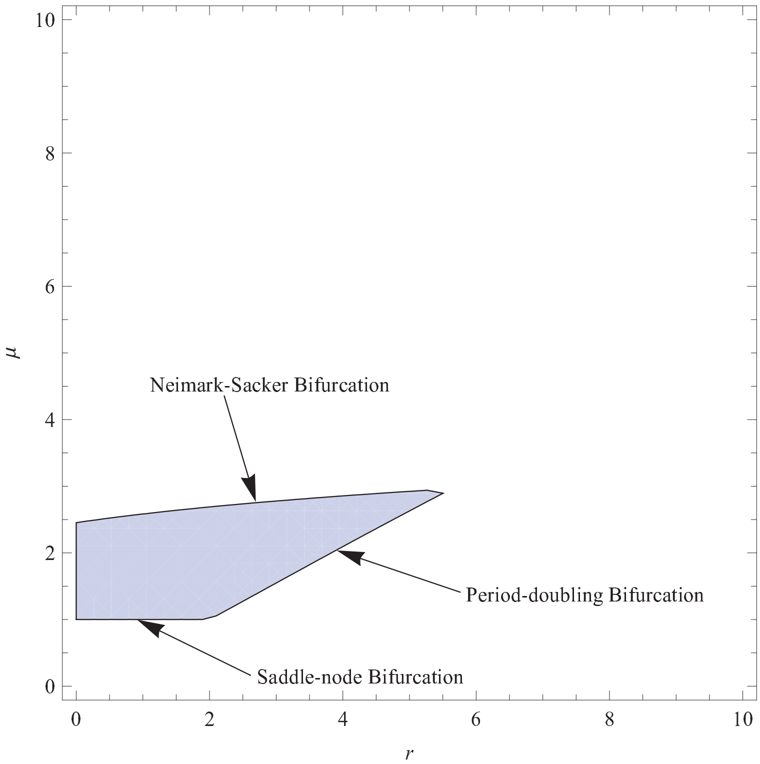

Figure 4.12: Types of bifurcation on the borderline of the stability region. $q = 1.6$.

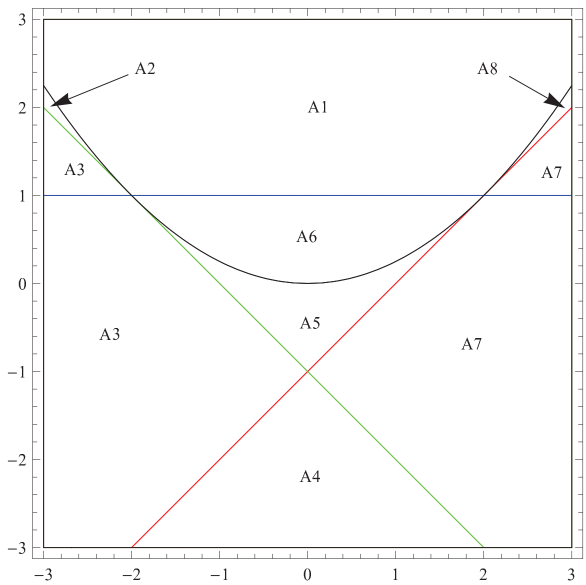

Figure 4.13: Tr-Det Diagram for general 2-dimensional discrete-time system.

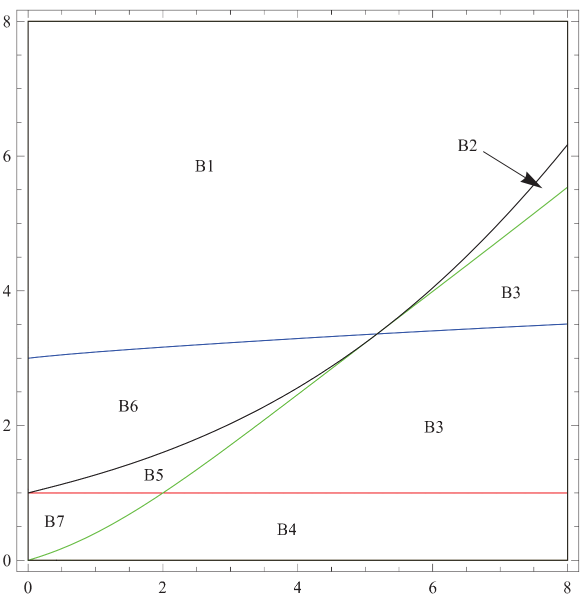

Figure 4.14: Corresponding regions for system (4.2).

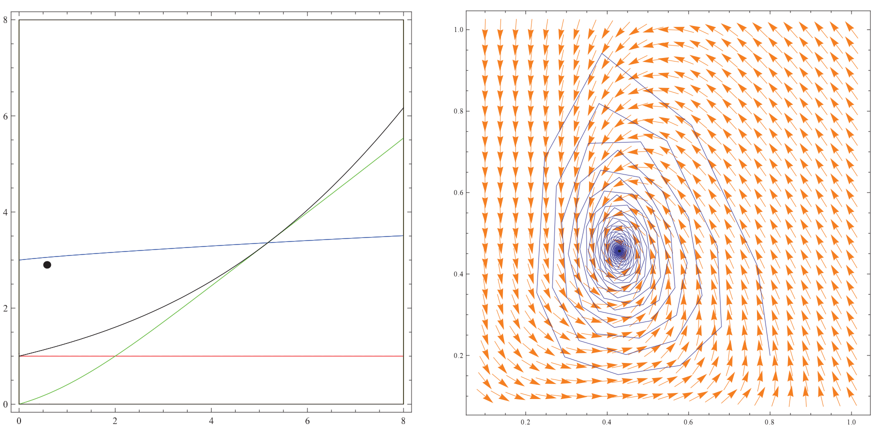

(a) Bifurcation Diagram (b) Phase Diagram

Figure 4.15: (r, μ) is inside the stability region.

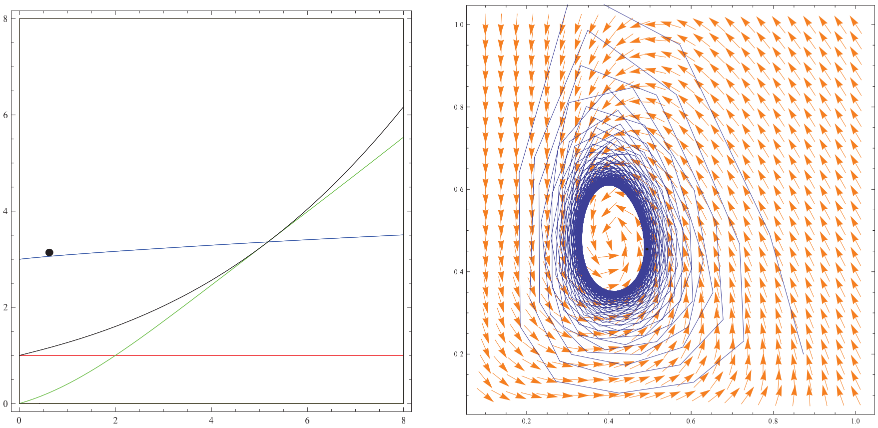

(a) Bifurcation Diagram (b) Phase Diagram

Figure 4.16: (r, μ) is outside the stability region.

4.2 Beddington Model with Allee Effect

4.2.1 Allee Effect on Parasitoid Population

In this section, we investigate the Beddington model with Allee effect on the parasitoid population:

$$\begin{aligned} N_{t+1} &= N_t \exp\left[r\left(1-\frac{N_t}{K}\right)-aP_t\right], \\ P_{t+1} &= eN_t[1-\exp(-aP_t)]\frac{P_t}{A+P_t}, \end{aligned} \tag{4.19}$$

where the parameters r, K, a, e, and A are positive. Now, we eliminate some of the parameters by changing the variables. Taking $x_t = \frac{N_t}{K}$, and $y_t = aP_t$, we obtain

$$\begin{aligned} x_{t+1} &= x_t \exp\left[r\left(1-x_t\right)-y_t\right], \\ y_{t+1} &= mx_t[1-\exp(-y_t)]\frac{y_t}{B+y_t}, \end{aligned} \tag{4.20}$$

where $m = aeK$ and $B = aA$.

4.2.1.1 Equilibrium Points

The fixed points of the discrete system (4.20) are obtained:

Theorem 4.6 *Let*

$$F(x) = -r + (r+m)\,x - mx\exp\left[-r(1-x)\right]$$

and

$$\theta = \frac{(B+r)\sqrt{r} + \sqrt{B+r}\sqrt{4m + r(4+B+r)}}{2(m+r)}.$$

For the system given in (4.20),

a. for any values of parameters, there exist two non-negative fixed points which are $(0,0)$ *and* $(1,0)$*.*

b. there exist one positive fixed point $(\theta, r(1-\theta))$ *if and only if* $m > 1$ *and* $B = F(\theta)$*.*

c. there exist two positive fixed points in the form $(\ell, r(1-\ell))$*, if and only if* $m > 1$ *and* $B < F(\theta)$*, where* $0 < \ell < 1$*.*

Proof. To find the fixed points of the system given in (4.20), the following system of equations must be solved:

$$\begin{aligned} x &= x\exp\left[r\,(1-x) - y\right], \\ y &= mx[1-\exp(-y)]\frac{y}{B+y}. \end{aligned} \tag{4.21}$$

If $x = 0$, we have the extinction fixed point $(0,0)$. If $x \neq 0$ and $y = 0$ we obtain the exclusion fixed point $(1,0)$.

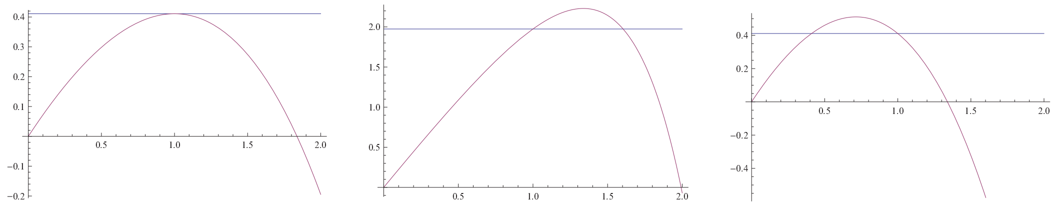

(a) $m = 1$ (b) $m < 1$ (c) $m > 1$

Figure 4.17: $z = F(x)$.

If $x \neq 0$ and $y \neq 0$ the system of equations (4.21) becomes

$$\begin{aligned} y &= r\,(1-x)\,, \\ x &= \frac{B+y}{m[1-\exp(-y)]}. \end{aligned} \tag{4.22}$$

Eliminating y in (4.22), we obtain

$$B = -r + (r+m)\,x - mx\exp\left[-r(1-x)\right]. \tag{4.23}$$

Let us denote $z = F(x) = -r + (r+m)\,x - mx\exp\left[-r(1-x)\right]$. When this curve intersects with the horizontal line $z = B$, some fixed points are obtained.

Notice that F is continuous, $F(0) = -r < 0$, $F(1) = 0$, $F''(x) < 0$ for all x, $\lim_{x\to\infty} F(x) = -\infty$, $F'(0) > 0$. Since $F'(1) = r(1-m)$, we have the following cases:

i. If $m = 1$, then $F'(1) = 0$ and the only maximum point is at $x = 1$. Since $B > 0$ there is no intersection of the functions $z = B$ and $z = F(x)$ (See Figure 4.17(a)).

   If $m < 1$, then $F'(1) > 0$. We know that $F''(x) < 0$ for all x and $\lim_{x\to\infty} F(x) = -\infty$. This means that, for some values of B there exist one (if the horizontal line is tangent to the curve $z = F(x)$) or two (if B is less than the height of the maximum point of the function $z = F(x)$) fixed points and for any of them if we denote the x-component of the fixed point by $x = \omega$, then $\omega > 1$. We have $y = r(1-\omega) < 0$ by the first equation of system (4.22) (See Figure 4.17(b)). Since one component of $(\omega, r(1-\omega))$ is negative, this fixed point is not of interest in biology and hence it will be omitted.

ii. If $m > 1$, then $F'(1) < 0$. We know that $F''(x) < 0$ for all x and $F(0) = -r < 0$. Hence, for some values of B there exist one (if the horizontal line is tangent to the curve $z = F(x)$) or two (if B is less than the height of the maximum point of the function $z = F(x)$) fixed points. Let us denote the x-component of this fixed point by $x = \ell$. Then $\ell < 1$ and hence $y = r(1-\ell) > 0$ by (4.22) (See Figure 4.17(c)). Hence, $(\ell, r(1-\ell))$ is a candidate to be a coexistence fixed point.

Now, we have to determine that in which condition the horizontal line $z = B$ intersects the function $z = F(x)$ for $m > 1$. That is the condition when the number B is less than the height of the maximum value of the curve $z = F(x)$. Let us denote the maximum point by $(\bar{x}, \bar{y})$. In order to find that point, we have

$$F'(\bar{x}) = r - m\left(-1 + e^{r(-1+\bar{x})}(1 + r\bar{x})\right) = 0.$$

We focus on the case where the horizontal line $z = B$ is tangent to the curve $z = F(x)$, that is $F(\bar{x}) = B$:

$$-r + (r+m)\,x - mx \exp\left[-r(1-x)\right] = B.$$

Eliminating the term $e^{r(1-\bar{x})}$ in the two equations above, we obtain

$$-r + (m+r)\bar{x} - \frac{(m+r)\bar{x}}{1 + r\bar{x}} = B. \tag{4.24}$$

The positive solution of equation (4.24) for $\bar{x}$ is as follows:

$$\bar{x} = \frac{(B+r)\sqrt{r} + \sqrt{B+r}\sqrt{4m + r(4+B+r)}}{2(m+r)}. \tag{4.25}$$

Hence, the condition for existence of the positive fixed point in part (b) and (c) is obtained: There exist one intersection point $(\bar{x}, r(1-\bar{x}))$ if and only if $m > 1$ and $B = F(\bar{x})$. And there exist two intersection points if and only if $m > 1$ and $B < F(\bar{x})$.

□

4.2.1.2 Stability of Fixed Points for System (4.20)

Theorem 4.7 *For system (4.20), the following statements hold true:*

a. $(0,0)$ *is unstable.*

b. if $0 < r \leq 2$*, then* $(1,0)$ *is asymptotically stable .*

Proof. The Jacobian matrix of the map

$$G(x,y) = \left(xe^{r(1-x)-y}, mx(1-e^{-y})\frac{y}{B+y}\right)$$

is

$$JG(x,y) = \begin{pmatrix} e^{r-rx-y}(1-rx) & -e^{r-rx-y}x \\ \frac{(1-e^{-y})my}{B+y} & \frac{e^{-y}mx\left(y^2+B(-1+e^y+y)\right)}{(B+y)^2} \end{pmatrix}.$$

a. The Jacobian evaluated at the point $(0,0)$ is

$$JG(0,0) = \begin{pmatrix} e^r & 0 \\ 0 & 0 \end{pmatrix}.$$

The eigenvalues of $JG(0,0)$ are 0 and e^r. Since $r > 0$, $e^r > 1$. Thus $(0,0)$ is unstable. We also notice that any point with the form $(0,y)$ is eventually fixed point, because starting with $(0,y)$, we get $(0,0)$ after one iteration.

b. The Jacobian evaluated at $(1,0)$ is

$$JG(1,0) = \begin{pmatrix} 1-r & -1 \\ 0 & 0 \end{pmatrix}.$$

The eigenvalues for this matrix are $\lambda_1 = 1 - r$ and $\lambda_2 = 0$. Thus, the fixed point $(1,0)$ is locally asymptotically stable if $\rho(JG(1,0)) < 1$, that is $0 < r < 2$. If $r > 2$, the fixed point $(1,0)$ is unstable. If $r = 2$, then the eigenvalue are $\lambda_1 = -1$ and $\lambda_2 = 0$. Now, we have to apply the center manifold theorem [13]: by changing variables, let $u = x - 1$ and $v = y$ in system (4.20), we have a shift from the point $(1,0)$ to $(0,0)$. Then the new system is given by

$$\begin{aligned} u_{t+1} &= (u_t + 1)\exp\left[-ru_t - v_t\right] - 1, \\ v_{t+1} &= m(u_t+1)[1 - \exp(-v_t)]\frac{v_t}{B+v_t}. \end{aligned} \tag{4.26}$$

The Jacobian of the planar map given in (4.26) is

$$\tilde{J}G(u,v) = \left(\begin{array}{cc} -e^{-ru-v}(-1+r+ru) & -e^{-ru-v}(1+u) \\ \frac{\left(1-e^{-v}\right)mv}{B+v} & \frac{e^{-v}m(1+u)\left(v^2+B(-1+e^v+v)\right)}{(B+v)^2} \end{array} \right). \tag{4.27}$$

At $(0,0)$, $\tilde{J}G$ has the form

$$\tilde{J}G(0,0) = \begin{pmatrix} 1-r & -1 \\ 0 & 0 \end{pmatrix}.$$

When $r = 2$ we have

$$\tilde{J}G(0,0) = \begin{pmatrix} -1 & -1 \\ 0 & 0 \end{pmatrix}.$$

Now we can write the equations in system (4.26) as

$$\begin{aligned} u_{t+1} &= -u_t - v_t + \tilde{f}(u_t, v_t), \\ v_{t+1} &= \tilde{g}(u_t, v_t), \end{aligned} \tag{4.28}$$

where

$$\tilde{f}(u_t, v_t) = -1 + u_t + e^{-2u_t - v_t}(1 + u_t) + v_t$$

and

$$\tilde{g}(u_t, v_t) = \frac{(1 - e^{-v_t})\, m(1 + u_t)v_t}{B + v_t}.$$

By Theorem 2.9, let us assume that the map $v = h(u)$ takes the form

$$h(u) = \alpha u^2 + \beta u^3 + O(u^4), \quad \alpha, \beta \in \mathbb{R}.$$

Now, we are going to compute the constants α and β. The function $v = h(u)$ must satisfy the center manifold equation

$$h\left[-u - h(u) + \tilde{f}(u, h(u))\right] - \tilde{g}(u, h(u)) = 0.$$

The Taylor series expansion at the point $u = 0$ is evaluated for the equation above. Equating the coefficients of the series, we obtain $\alpha = \beta = 0$.

Thus on the center manifold $v = 0$ we have the following map

$$P(u) = -1 + e^{-2u}(1 + u).$$

Calculations show that $P'(0) = -1$ and Schwarzian derivative of the map Q at the origin is $-\frac{4}{3} < 0$. Hence, the exclusion fixed point $(1, 0)$ is locally asymptotically stable (See Figure 4.18).

□

4.2.1.3 Stable and Unstable Manifolds

For the point $(0, 0)$, since $|\lambda_1| = e^r > 1$ and $|\lambda_2| = 0 < 1$, the extinction fixed point is saddle for any values of parameters r and m. For this point, x axis is unstable and y axis is stable manifold.

Now, let us focus on the exclusion fixed point, $(1, 0)$: By using the similar procedure that is used for the center manifold in the proof of Theorem 4.7, we obtain

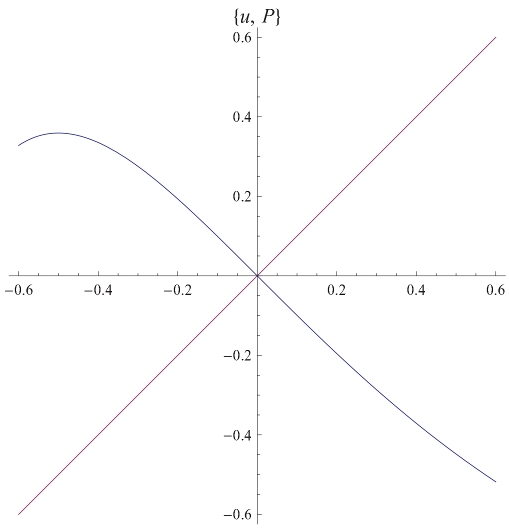

Figure 4.18: The map P on the center manifold $v = h(u)$.
$r = 2$.

the stable and unstable manifolds. In model (4.20) the saddle scenario for the exclusion fixed point occurs when $r > 2$. Shifting the exclusion fixed point from $(1, 0)$ to $(0, 0)$, we have the following Jacobian matrix:

$$\tilde{J}G(0,0) = \begin{pmatrix} 1-r & -1 \\ 0 & 0 \end{pmatrix}.$$

We can write the equations in system (4.26) as

$$\begin{aligned} u_{t+1} &= -1u_t - v_t + \tilde{f}(u_t, v_t), \\ v_{t+1} &= \tilde{g}(u_t, v_t), \end{aligned} \tag{4.29}$$

where

$$\tilde{f}(u_t, v_t) = -1 + (-1+r)u + e^{-ru-v}(1+u) + v$$

and

$$\tilde{g}(u_t, v_t) = \frac{(1-e^{-v})\, m(1+u)v}{B+v}.$$

The eigenvalues of the Jacobian matrix $\tilde{J}G(0,0)$ are $\lambda_1 = 1 - r$ and $\lambda_2 = 0$. Thus, at the fixed point $(1, 0)$, the unstable and stable manifold must be tangent to the eigenvectors $\begin{pmatrix} 1 \\ 0 \end{pmatrix}$ and $\begin{pmatrix} 1 \\ 1-r \end{pmatrix}$, respectively.

In order to find the unstable manifold for the exclusion fixed point, we assume that the map $v = h(u)$ takes the form

$$h(u) = \alpha u^2 + \beta u^3 + O(u^4), \quad \alpha, \beta \in \mathbb{R}.$$

The map h must satisfy the following center manifold equation

$$h\Big((1-r)u - h(u) + \tilde{f}(u, h(u))\Big) - \tilde{g}(u, h(u)) = 0.$$

The Taylor expansion at the point $(0, 0)$ yields

$$\alpha(-1+r)^2u^2 - (-1+r)\left(-2\alpha^2 + \beta(-1+r)^2 + \alpha(-2+r)r\right)u^3 + O[u]^4 = 0.$$

Thus, we obtain $\alpha = \beta = 0$. Hence, the unstable manifold is $h(u) = 0$ and the map on the unstable manifold is

$$Q(u) = -1 + e^{-ru}(1+u).$$

Notice that $|Q'(0)| = |1-r| > 1$ when $r > 2$.

In order to find the stable manifold for the exclusion fixed point, we assume that map h takes the form

$$h(v) = \frac{1}{1-r}v + \alpha v^2 + \beta v^3 + O(v^4), \quad \alpha, \beta \in \mathbb{R}.$$

Hence, the center manifold equation is

$$h\left(\tilde{g}(h(v), v)\right) - (1-r)h(v) + v - f(\tilde{h(v)}, v) = 0.$$

By using the Taylor series expansion at the point $(0,0)$ and equating the coefficient of the polynomials to 0, we obtain

$$\alpha = \frac{2m + B(-3+r)}{2B(-1+r)^2}$$

and

$$\beta = -\frac{6m(-1+r)^2 + 3Bm(-1+r)^2 + B^2\left(-9+21r-9r^2+r^3\right)}{6B^2(-1+r)^4}.$$

Hence, the map on the center manifold is obtained as

$$R(v) = \frac{\left(1-e^{-v}\right) mv \left(1 + \frac{v}{1-r} + \alpha v^2 + \beta v^3\right)}{B+v},$$

and the stable manifold is

$$h(v) = \frac{v}{1-r} + \alpha v^2 + \beta v^3,$$

where α and β are given above. Notice that $R'(0) = 0$ which makes the fixed point $(1,0)$ locally asymptotically stable (See Figure 4.19).

Figure 4.20 represents the Beddington model without Allee effect ($B = 0$). With the given parameters, the coexistence fixed point exists and is locally asymptotically stable. Increasing the Allee effect constant B from 0 to 0.13, a new coexistence fixed point appears and exclusion fixed points becomes locally stable. See Figure 4.21. Furthermore, with the parameter $B = 0.3$, the coexistence fixed point disappears due to the Allee effect, hence the parasitoid population extinct. See Figure 4.22.

4.2.2 Allee Effect on Host Population

In [22], the authors investigated the following model. The model is Beddington model with the host subject to an Allee effect:

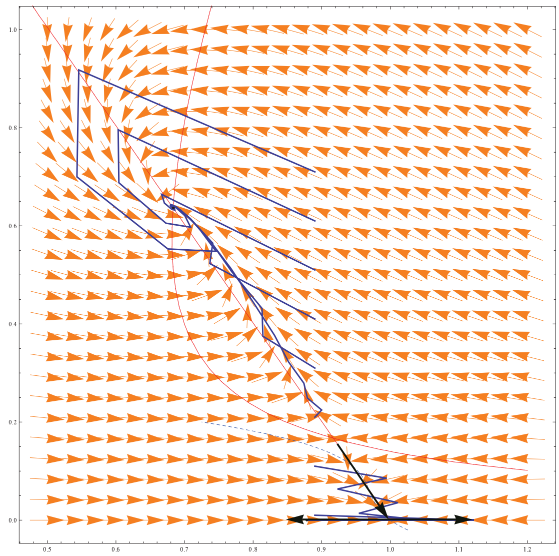

Figure 4.19: Stable and unstable manifolds for the fixed point $(1, 0)$. $m = 2.6$, $B = 0.2$, and $r = 2.01$. The dashed curve represents the stable manifold. Two isocline curves are also presented.

$$\begin{aligned} N_{t+1} &= N_t \exp\left[r\left(1 - \frac{N_t}{K}\right) - aP_t\right] \frac{N_t}{A + N_t}, \\ P_{t+1} &= eN_t[1 - \exp(-aP_t)], \end{aligned} \tag{4.30}$$

where the parameters r, K, a, A, and e is positive.

In this section, we analyse the following discrete-time model which is the generalization of model (4.30):

$$\begin{aligned} N_{t+1} &= N_t \exp\left[r\left(1 - \frac{N_t}{K}\right) - aP_t\right] \frac{N_t}{A + N_t}, \\ P_{t+1} &= eN_t[1 - \exp(-bP_t)], \end{aligned} \tag{4.31}$$

where the parameters r, K, a, A, e, and b are positive.

Now, we eliminate some of the parameters by changing the variables. Taking

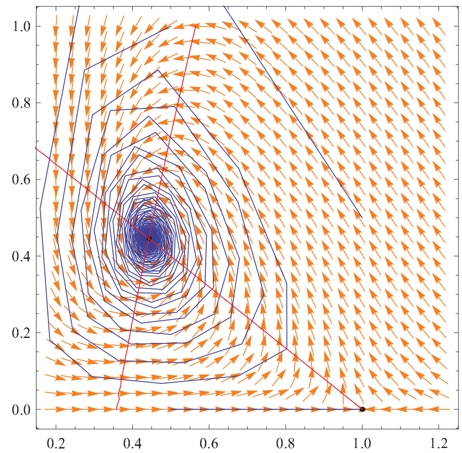

Figure 4.20: The system without Allee effect.
$m = 2.8$, $B = 0$, and $r = 0.8$. The curves represent the isoclines.

$x_t = \frac{N_t}{K}$, and $y_t = bP_t$, we obtain

$$\begin{aligned} x_{t+1} &= x_t \exp\left[r\left(1 - x_t\right) - qy_t\right] \frac{x_t}{B + x_t}, \\ y_{t+1} &= mx_t[1 - \exp(-y_t)], \end{aligned} \tag{4.32}$$

where $m = beK$, $q = \frac{a}{b}$, and $B = \frac{A}{K}$.

4.2.2.1 Equilibrium Points

In this section, we analyse the fixed points of discrete system (4.32). Firstly, we have to focus on the following isocline equations:

$$\begin{aligned} x &= x \exp\left[r\left(1 - x\right) - qy\right] \frac{x}{B + x}, \\ y &= mx[1 - \exp(-y)]. \end{aligned} \tag{4.33}$$

Extinction and Exclusion Fixed points

In equation (4.33), if $x = 0$, we have the extinction fixed point
$P_1^* = (x_1^*, y_1^*) = (0, 0)$.

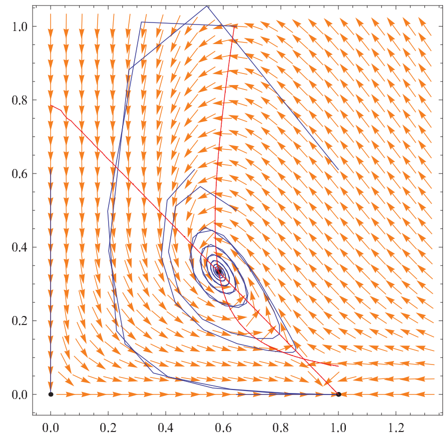

Figure 4.21: The system with Allee effect.
$m = 2.8$, $B = 0.13$, and $r = 0.8$. Both exclusion and a coexistence fixed point are locally asymptotically stable. The curves represent the isoclines.

In order to find the exclusion fixed points, we take $x \neq 0$ and $y = 0$ in system of equations (4.33). Hence, we obtain

$$B = x\left(e^{r(1-x)} - 1\right). \tag{4.34}$$

Let us denote $z = F(x) = x\left(e^{r(1-x)} - 1\right)$. When this curve intersects with the horizontal line $z = B$, some fixed points are obtained.
Notice that F is contiuous, $F(0) = F(1) = 0$, $F'(0) > 0$, $\lim_{x\to\infty} F(x) = -\infty$ and there is a unique x such that $F'(x) = 0$, where $x \in (0, 1)$.
Now, we have to determine that in which condition the horizontal line $z = B$ intersects the function $z = F(x)$. That is the condition when the number B is less than the height of the maximum value of the curve $z = F(x)$. Let us denote the maximum point by $(\bar{x}, \bar{y})$. In order to find that point, we have

$$F'(\bar{x}) = e^{r(1-\bar{x})}(1 - r\bar{x}) - 1 = 0. \tag{4.35}$$

We focus on the case where the horizontal line $z = B$ is tangent to the curve $z = F(x)$, that is $F(\bar{x}) = B$:

$$\bar{x}\left(e^{r(1-\bar{x})} - 1\right) = B. \tag{4.36}$$

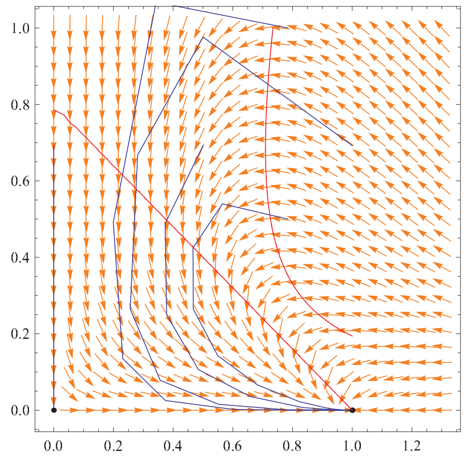

Figure 4.22: The system with Allee effect.
$m = 2.8$, $B = 0.3$, and $r = 0.8$. No coexistence fixed points. The Allee effect is so strong that the parasitoid population extinct. The curves represent the isoclines.

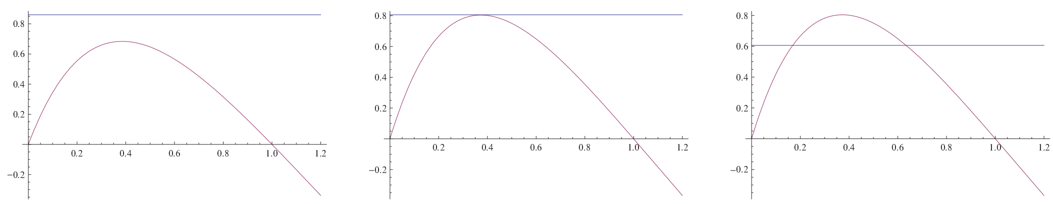

(a) $B > F(\theta)$ (b) $B = F(\theta)$ (c) $B < F(\theta)$

Figure 4.23: $z = F(x)$, $z = B$.

Eliminating the term $e^{r(1-\bar{x})}$ in equations (4.35) and (4.36), we obtain

$$r\bar{x}^2 + Br\bar{x} - B = 0. \tag{4.37}$$

The positive solution of equation (4.37) for $\bar{x}$ is as follows:

$$\bar{x} = \frac{1}{2}\left[-B + \sqrt{B^2 + \frac{4B}{r}}\right]. \tag{4.38}$$

Hence, the condition for the existence of the exclusion fixed points is obtained: There exist no fixed points if $B > F(\bar{x})$; there exist only one fixed points if $B = F(\bar{x})$; and there exist two exclusion fixed points if $B < F(\bar{x})$. Furthermore, since $B > 0$ and function F is positive only on the interval $(0, 1)$, the

intersections always occur on this interval, from which we conclude that for the exclusion fixed points, say $P_2^* = (x_2^*, y_2^*)$ and $P_3^* = (x_3^*, y_3^*)$, we have $0 < x_2^* < 1$ and $0 < x_3^* < 1$. See Figure 4.23.
Hence, we obtain the following result:

Theorem 4.8 *Let*

$$F(x) = x\left(\exp\left[r(1-x)\right] - 1\right)$$

and

$$\theta = \frac{1}{2}\left[-B + \sqrt{B^2 + \frac{4B}{r}}\right].$$

For the system given in (4.32),

a. *for any values of parameters, there exists extinction fixed point* $(0,0)$.

b. *there exist no exclusion fixed points if* $B > F(\theta)$.

c. *there exists one exclusion fixed point* $(\theta, 0)$ *if* $B = F(\theta)$.

d. *there exist two exclusion fixed points if* $B < F(\theta)$.

Notice that the exclusion fixed points are obtained by taking $y = 0$, which vanishes the second equation of system (4.33), and solving the first equation. We give the graphs of the isoclines in Figure 4.24 with some values of parameters which confirms our results in the theorem. In Figure 4.24, $B = .5$ and the values for $F(\theta)$ are as follows: (a) $F(\theta) = 0.372 < B$, (b) $F(\theta) = 0.499 \approx B$, (c) $F(\theta) = 0.773 > B$.

Coexistence fixed points

Since we have more complicated non-algebraic equations for the isoclines, it is not easy to obtain a similar condition for the positive fixed points. However, we investigate this points numerically and find that for particular values of parameters there may exist zero, one or two positive fixed points. Figure 4.25 represents the possible numbers of coexistence fixed points.
Notice that, since

$$y'' = \frac{1}{q}\left[\frac{1}{(B+x)^2} - \frac{1}{x^2}\right] < 0$$

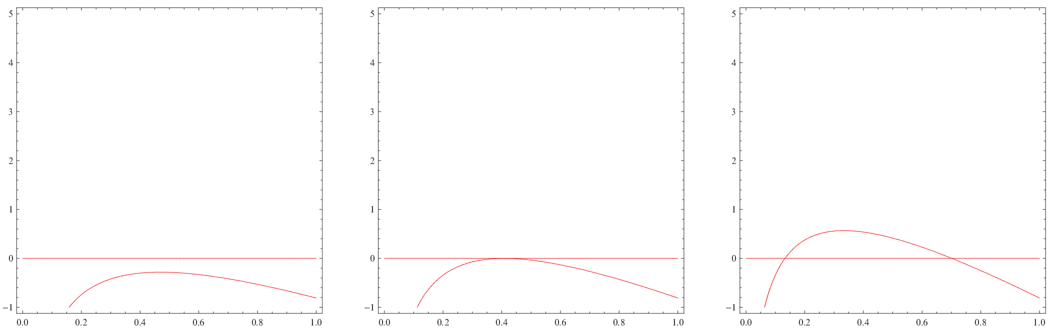

(a) $B > F(\theta)$ (b) $B = F(\theta)$ (c) $B < F(\theta)$

Figure 4.24: Isoclines of the system.
The horizontal line is the part of the isocline whose equation is the second equation of the system (4.33). The graph of the first equation is given by the curve. (a) $m = .1$, $B = .5$, $q = .5$, $r = 1.1$; (b) $m = .1$, $B = .5$, $q = .5$, $r = 1.35$; (c) $m = .1$, $B = .5$, $q = .5$, $r = 1.8$.

for the first equation in (4.33), first isocline is concave down, thus the only interval where the curve is above the x axis is (x_2^*, x_3^*). Hence, if a positive fixed point (x_+^*, y_+^*) exists, then it satisfies the condition $x_2^* < x_+^* < x_3^*$.
Furthermore, since $\theta = \theta(B, r)$ and $F(x)$ in Theorem 4.8 doesn't depend on the parameters q and m, we can conclude that the existence of any kind of fixed point does not depend on the parameters m and q. Even this parameters do not change the position of the exclusion fixed points. However, the existence and the position of the coexistence fixed points are affected by each of the parameters. Figure 4.26 represents the effect of the parameter q. For large values of m, the parameter q affects the existence of the positive fixed points. However, for a moderate values of m, where $x_2^* < \frac{1}{m} < x_3^*$, the parameter q does not affect the existence nor the number of positive fixed points but the positions of them. See Figure 4.27.
For a positive fixed point x_+^*, since $x_+^* < x_3^* < 1$ and the x-intercept of the second isocline is $\frac{1}{m}$ for $m < 1$, the isoclines do not intersect, hence there are no coexistence fixed points for this case. Of course, the inverse of this statement is not true. For example, see Figure 4.25 (a), for which $m = 2.5 > 1$ and there are no positive fixed points.

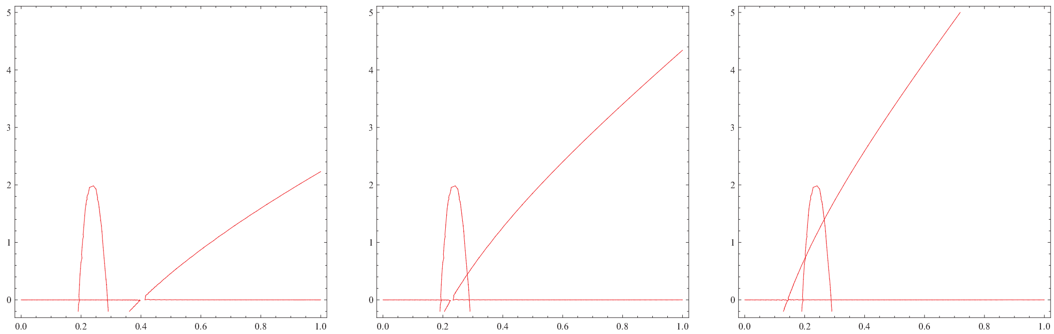

(a) no coexistence fixed points

(b) one coexistence fixed point

(c) two coexitence fixed points

Figure 4.25: Isoclines of the system.
(a) $m = 2.5$, $B = 4.75$, $q = .01$, $r = 4.02$; (b) $m = 4.4$, $B = 4.75$, $q = .01$, $r = 4.02$; (c) $m = 7$, $B = 4.75$, $q = .01$, $r = 4.02$.

4.2.2.2 Stability of Fixed Points for System (4.32)

In this section, we analyse the stability of fixed points for system (4.32).
Let

$$F(x) = x\left(\exp\left[r(1-x)\right] - 1\right) \tag{4.39}$$

and

$$\theta = \frac{1}{2}\left[-B + \sqrt{B^2 + \frac{4B}{r}}\right]. \tag{4.40}$$

Case 1. $B > F(\theta)$

Theorem 4.9 *For system (4.32), when $B > F(\theta)$, extinction fixed point $(0, 0)$ is globally asymptotically stable.*

Proof. With the assumption $B > F(\theta)$, the only fixed point is $(0, 0)$.
Furthermore, if $B > F(\theta)$, then $B > F(x_n)$ for any x_n.
If we start with (x_n, y_n), where $x_n = 0$ and $y_n \geq 0$, then $x_{n+1} = y_{n+1} = 0$.
Now, let us start with a point (x_n, y_n), where $x_n > 0$ and $y_n \geq 0$, and show that $x_{n+1} < x_n$ and $y_{n+1} < y_n$. Hence, proving the inequalities, the sequences must converge to the only fixed point $(0, 0)$:

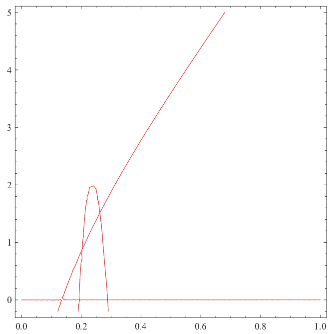

(a) two coexistence fixed points

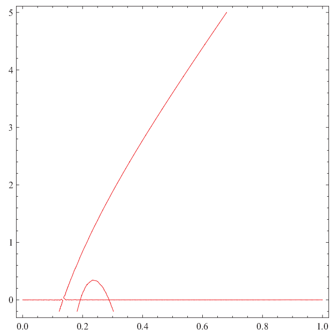

(b) no coexistence fixed points

Figure 4.26: The effect of the parameter q.
The parameter q affects the existence of the positive fixed points if m is large enough.(a) $m = 7.4$, $B = 4.75$, $q = .01$, $r = 4.02$; (b) $m = 7.4$, $B = 4.75$, $q = .06$, $r = 4.02$.

$$\begin{aligned} x_{n+1} &= x_n \exp[r(1-x_n) - qy_n]\tfrac{x_n}{B+x_n} \\ &\leq x_n \exp[r(1-x_n)]\tfrac{x_n}{B+x_n} \\ &< (B+x_n)\tfrac{x_n}{B+x_n} \\ &= x_n. \end{aligned}$$

Hence, $x_n \to 0$ as $n \to \infty$.

We also know that $y_{n+1} = mx_n(1-e^{-y_n}) < mx_n$, from which we conclude that $y_n \to 0$ as $x_n \to 0$. □

Case 2. $B = F(\theta)$ Now, for system (4.32), we are going to analyse the fixed point $(\theta, 0)$ when $B = F(\theta)$.

The Jacobian matrix of the map

$$G(x,y) = \left(xe^{r(1-x)-qy}\frac{x}{B+x}, mx(1-e^{-y}) \right)$$

is

$$JG(x,y) = \begin{pmatrix} -\frac{e^{r-rx-qy}x(B(-2+rx)+x(-1+rx))}{(B+x)^2} & -\frac{e^{r-rx-qy}qx^2}{B+x} \\ m - e^{-y}m & e^{-y}mx \end{pmatrix}.$$

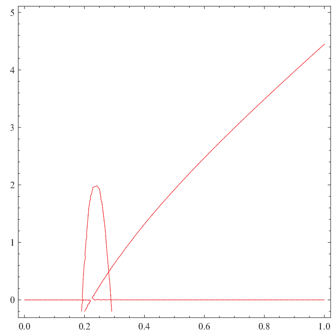

(a) one coexistence fixed point

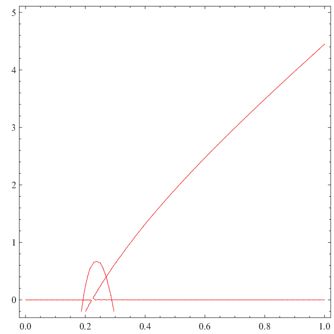

(b) one coexistence fixed point

Figure 4.27: The effect of the parameter q.
The parameter q does not affect the number of positive fixed points but the positions of them if $x_2^* < \frac{1}{m} < x_3^*$. (a) $m = 4.5$, $B = 4.75$, $q = .01$, $r = 4.02$; (b) $m = 4.5$, $B = 4.75$, $q = .03$, $r = 4.02$.

The Jacobian evaluated at the point $(\theta, 0)$ is

$$JG(\theta, 0) = \begin{pmatrix} -\frac{e^{r-r\theta}\theta(B(-2+r\theta)+\theta(-1+r\theta))}{(B+\theta)^2} & -\frac{e^{r-r\theta}q\theta^2}{B+\theta} \\ 0 & m\theta \end{pmatrix},$$

where θ is given in equation (4.40). By using equations (4.39) and (4.40), after some calculations, we obtain the following Jacobian matrix for the exclusion fixed point $(\theta, 0)$:

$$JG(\theta, 0) = \begin{pmatrix} 1 & -q\theta \\ 0 & m\theta \end{pmatrix}.$$

Hence, the fixed point $(\theta, 0)$ is non-hyberbolic.
The eigenvalues of $JG(\theta, 0)$ are $\lambda_1 = 1$ and $\lambda_2 = m\theta$. If $m\theta > 1$, then fixed point $(\theta, 0)$ is unstable. If $m\theta < 1$, then in order to investigate the stability of fixed points for this case, we have to apply the center manifold theory [13].
It is more convenient to make a change of variables in system (4.32) so we can have a shift from the point $(\theta, 0)$ to $(0, 0)$. Let $u = x - \theta$ and $v = y$. Then the

new system is given by

$$u_{t+1} = \frac{e^{r-qv_t-r(u_t+\theta)}(u_t+\theta)^2}{B+u_t+\theta} - \theta,$$
$$v_{t+1} = \mu(u_t+\theta)[1-\exp(-v_t)]. \tag{4.41}$$

At the point $(0,0)$, the Jacobian of the planar map given in (4.41) is

$$\tilde{J}G(0,0) = \begin{pmatrix} 1 & -q\theta \\ 0 & m\theta \end{pmatrix}.$$

Now we can write the equations in system (4.41) as

$$u_{t+1} = u_t - q\theta v_t + \tilde{f}(u_t, v_t),$$
$$v_{t+1} = m\theta v_t + \tilde{g}(u_t, v_t), \tag{4.42}$$

where

$$\tilde{f}(u_t, v_t) = -u_t - \theta + qv_t\theta + \frac{e^{-ru_t-qv_t}(B+\theta)(u_t+\theta)^2}{\theta(B+u_t+\theta)}$$

and

$$\tilde{g}(u_t, v_t) = -mv_t\theta + \left(1-e^{-v_t}\right)m(u_t+\theta).$$

By Theorem 2.9, let us assume that the map h takes the form

$$h(u) = \alpha u^2 + \beta u^3 + O(u^4), \quad \alpha, \beta \in \mathbb{R}.$$

Now we have to compute the constants α and β. The function h must satisfy the center manifold equation

$$h(u - q\theta h(u) + \tilde{f}(u, h(u))) - m\theta h(u) - \tilde{g}(u, h(u)) = 0.$$

The Taylor series expansions, at the point $u = 0$, are evaluated for the equation above. Equating the coefficients of the series and using the equations (4.39) and (4.40), after some manipulations, we obtain $\alpha = \beta = 0$.

Thus on the center manifold $v = h(u)$, we find the following map

$$P(u) = -\theta + \frac{e^{-r(-1+u+\theta)}(u+\theta)^2}{B+u+\theta},$$

where θ is given in equation (4.40).
Calculations show that $P'(0) = 1$ and

$$P''(0) = -\frac{B^2\left(4 + Br + r\sqrt{\frac{B(4+Br)}{r}}\right)}{r\left(-B + \sqrt{\frac{B(4+Br)}{r}}\right)} < 0.$$

Hence, for the map P, the origin is semistable from the right. See Figure 4.28.
Notice that this result is valid when $m\theta < 1$ which yields the condition
$r > \frac{Bm^2}{1+Bm}$.

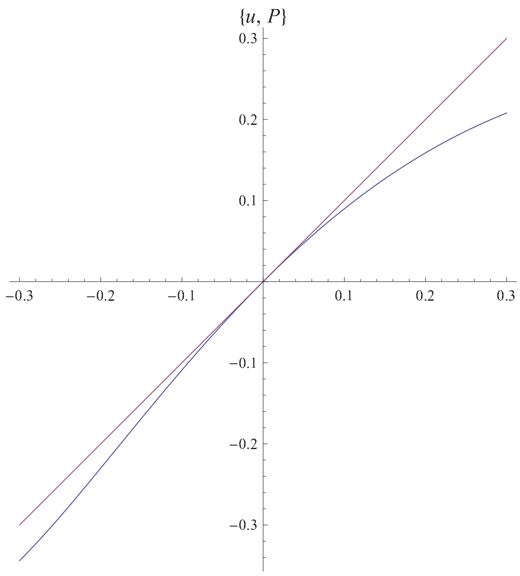

Figure 4.28: Map P on the center manifold $v = h(u)$.
$(0, 0)$ is semi-stable from the right. $B = .500$ and $r = 1.351$.

Now, we are going to find the stable manifold, which exists when $m\theta < 1$. Since the stable manifold is tangent to the eigenvector at the point, let us take

$$h(v) = \frac{q\theta}{m\theta - 1}v + \alpha v^2 + \beta v^3.$$

This map must satisfy the center manifold equation

$$h(m\theta v + \tilde{g}(h(v), v)) - h(v) + q\theta v - \tilde{f}(h(v), v) = 0.$$

We calculate map Q on the stable manifold and found that $Q'(0) = m\theta$, which is expected. Because of the long output of the computations we omit them here. Figure 4.29 shows the map Q.
Stable and center manifolds are given in Figure 4.30.

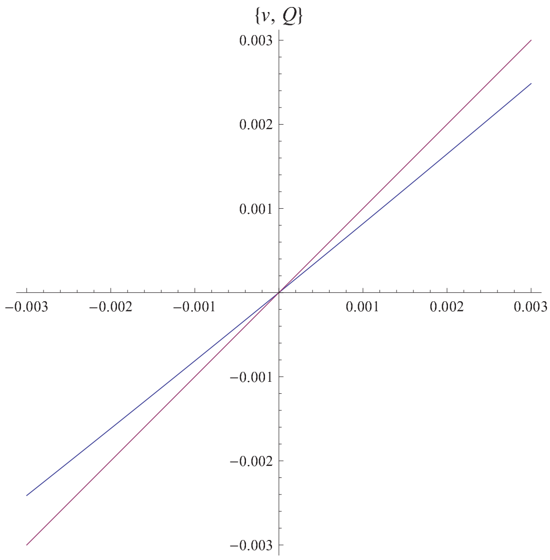

Figure 4.29: Map Q on the center manifold $u = h(v)$.
$(0, 0)$ is asymptotically stable. Notice that $m\theta < 1$. $B = .5$, $q = 1.1$, $m = 2$ and $r = 1.351$.

Case 3. $B < F(\theta)$ The dynamics of this case, for which there may exist zero, one, or two positive fixed points, is much more complicated due to the non-algebraic equations of the isoclines.
By symbolic/numeric computations we obtain the stability region of the exclusion fixed point when $B < F(\theta)$. Figure 4.31 represents the stability region for the exclusion fixed point P_3^* on the r-m parameter space. In Figure 4.32, we give the phase diagram of the system when there exist no positive fixed point. In Figure 4.33, the phase diagram represents the dynamics of the system when there exists a positive fixed point and for the given values of parameters, the positive fixed point is asymptotically stable.

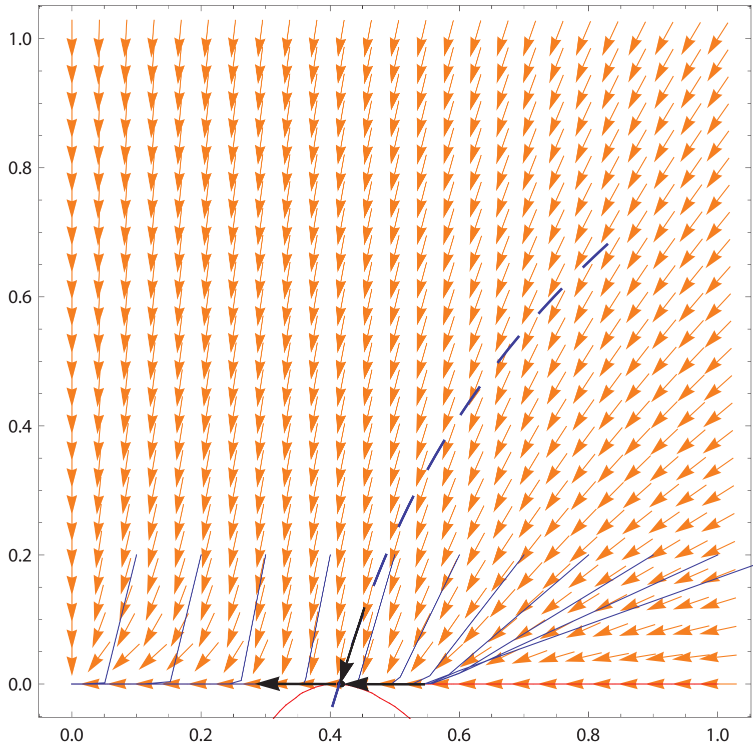

Figure 4.30: Invariant manifolds.
The phase diagram showing the stable and center manifolds when $B = F(\theta)$ and $m\theta < 1$. Semi-stability of fixed point for map P on the center manifold $v = h(u) = 0$ can be also seen. $m = .1$, $B = .5$, $q = .5$, and $r = 1.351$.

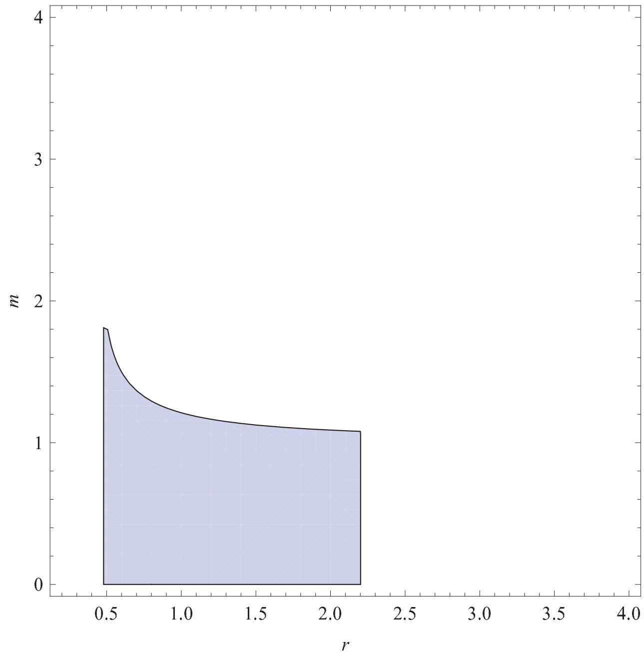

Figure 4.31: The estimated stability region of exclusion fixed point P_3^*. $B = 0.1$, $q = 0.6$.

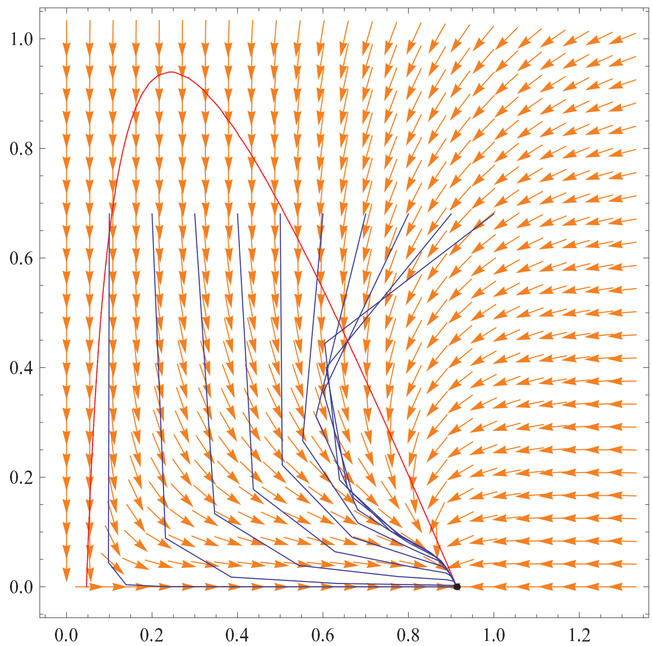

Figure 4.32: Phase diagram of the system when there are no positive fixed points. $m = .9$, $B = .1$, $q = .6$, and $r = 1.2$.

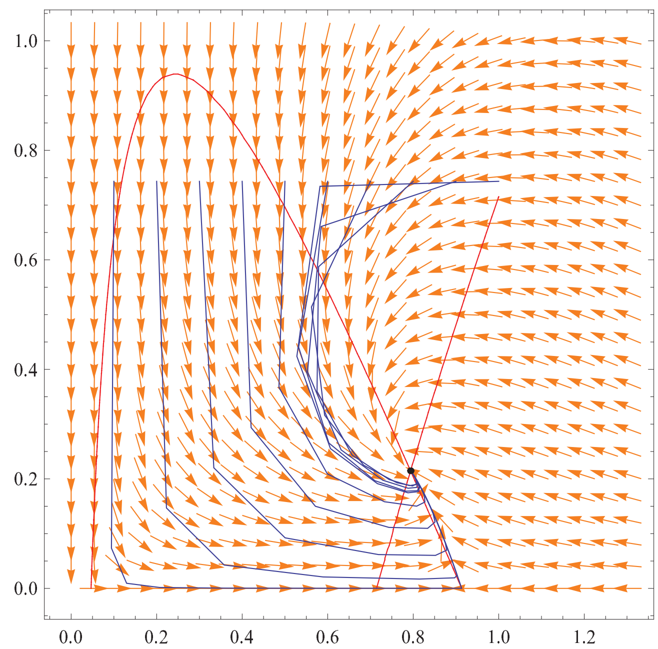

Figure 4.33: Phase diagram of the system when there exists a positive fixed point. $m = 1.4$, $B = .1$, $q = .6$ and $r = 1.2$.

Chapter 5

Conclusion and Further Studies

In this thesis, we investigated the stability and bifurcation of a generalized Beddington host-parasitoid model. We were able to study the stability of the coexistence fixed point without actually computing it. This is accomplished by using upper and lower sequences approaching the coexistence fixed point. By this, we have established the mathematical analysis and provided novel tools to study the stability of fixed points for the models where there is no explicit formula for the fixed points. Our results confirmed the known results in the literature for the special case $a = b$ that were obtained via simulation. The invariant manifolds for the extinction and exclusion fixed points were obtained. Due to the lack of an explicit formula of the coexistence fixed point, we were not able to investigate the Neimark-Sacker bifurcation and the other types of bifurcations. The presence of Neimark-Sacker bifurcation was shown via numerical simulations. Moreover, the global dynamics of the system has not been determined and needs further study.

We also investigated the Beddington model with the parasitoid subject to an Allee effect and the generalized Beddington model with the host subject to an Allee effect. We analysed the stability and invariant manifolds of both of the systems.

Appendix A

Mathematica Codes

In Appendix A, we present some of the *Mathematica* modules used during this thesis. We wrote and executed the codes on *Mathematica 7.0.0*. For each module, we give the code and a simple example of its usage.

A.1 Cobweb Diagram

Code

```
Cobweb[F_, t0_] :=
 Module[{ff, diagonal, funct, list, l, ldot, ttt, sonlist},
  ff[a_] := F /. x -> a;
  diagonal = Plot[x, {x, 0, 1}, PlotStyle -> Red];
  funct = Plot[F, {x, 0, 1}];
  list = Table[{Nest[ff, t0, n], Nest[ff, t0, n + 1]}, {n, 0, 100}];
  ldot = ListPlot[list];
  sonlist = {{t0, 0}};
  For[i = 1, i < 101, i++, sonlist = Append[sonlist, list[[i]]];
   sonlist =
    Append[sonlist, {sonlist[[2 i]][[2]], sonlist[[2 i]][[2]]}]];
```

```
  l = ListPlot[sonlist, Joined -> True];
  ttt = Graphics[{PointSize[Large], Pink, Point[Last[sonlist]]}];
  Show[ldot, funct, diagonal, l, ttt]
  ]
```

Example

```
Cobweb[3.2 x (1 - x), .88]
```

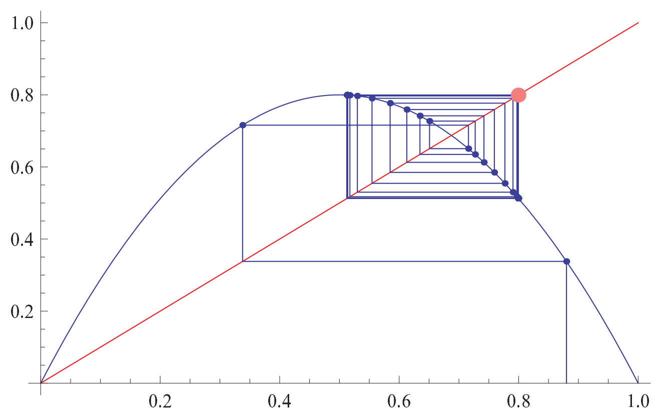

A.2 Time Series Diagram

Code

```
DDSPhasePlane1[fg_, varx_, vary_, x0_, y0_] :=
 Module[{F, G, X, Y, p0, lll},
  F[x_, y_] := fg[[1]] /. {varx -> x, vary -> y};
  G[x_, y_] := fg[[2]] /. {varx -> x, vary -> y};
  X[a_] := F[a[[1]], a[[2]]];
  Y[b_] := G[b[[1]], b[[2]]];
  p0 = {x0, y0};
  lll = NestList[{X[{#[[1]], #[[2]]}], Y[{#[[1]], #[[2]]}]} &, p0,
```

```
  100];
l1 = ListPlot[Transpose[lll][[1]], Joined -> True, PlotRange -> All];
l2 = ListPlot[Transpose[lll][[2]], Joined -> True,
  PlotStyle -> Orange];
Show[l1, l2]
]
```

Example

```
DDSPhasePlane1[{x + 2.9 x (1 - x) - 2 x y, 1.33 x y}, x, y, .8, .1]
```

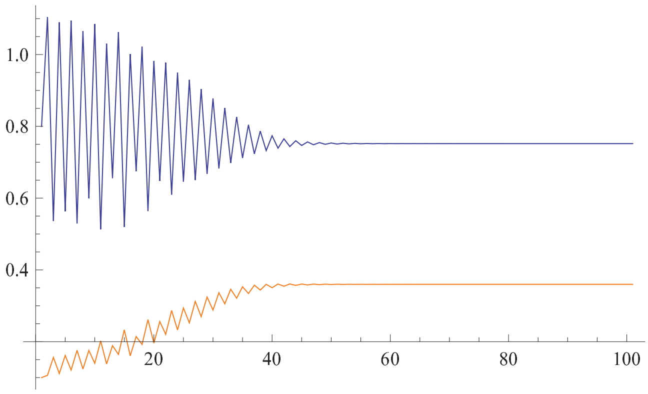

A.3 Phase Diagram

Code

```
DDynamicss[fg_, varx_, vary_, ss_, rr_] :=
 Module[{horizontalinitials, verticalinitials, x, y, ppvector, dyn,
   gr1, gr2},
  PtoPvector[fg1_, varx1_, vary1_, x01_, y01_] :=
   Module[{F, G, X, Y, p0, lll, lp, ttt},
    F[x_, y_] := fg1[[1]] /. {varx1 -> x, vary1 -> y};
```

```
  G[x_, y_] := fg1[[2]] /. {varx1 -> x, vary1 -> y};
  X[a_] := F[a[[1]], a[[2]]];
  Y[b_] := G[b[[1]], b[[2]]];
  p0 = {x01, y01}; q0 = {X[p0], Y[p0]}; q0 - p0
  ];
ppvector =
 VectorPlot[PtoPvector[fg, varx, vary, x, y], {x, 0, 1}, {y, 0, 1},
  VectorPoints -> Fine, VectorScale -> {Automatic, Automatic, None},
   VectorStyle -> Orange];
DDSPhasePlane2[fg2_, varx2_, vary2_, x02_, y02_, iterate_] :=
 Module[{F, G, X, Y, p0, lll, lp, ttt},
  F[x_, y_] := fg2[[1]] /. {varx2 -> x, vary2 -> y};
  G[x_, y_] := fg2[[2]] /. {varx2 -> x, vary2 -> y};
  X[a_] := F[a[[1]], a[[2]]];
  Y[b_] := G[b[[1]], b[[2]]];
  p0 = {x02, y02};
  lll =
   NestList[{X[{#[[1]], #[[2]]}], Y[{#[[1]], #[[2]]}]} &, p0,
    iterate];
  lp = ListPlot[lll, Joined -> True, AxesLabel -> {varx2, vary2},
    PlotRange -> All, PlotLabel -> {varx2, vary2}];
  Show[lp, Graphics[Point[Last[lll]]]]
  ];
dyn[xx0_, yy0_] := DDSPhasePlane2[fg, varx, vary, xx0, yy0, 1000];
horizontalinitials = Table[dyn[nx, rr], {nx, 0, 1, .2}];
verticalinitials = Table[dyn[ss, ny], {ny, 0, 1, .3}];
gr2 = ContourPlot[{varx == fg[[1]], vary == fg[[2]]}, {varx, 0,
   1}, {vary, 0, 1}, ColorFunction -> Hue];
Show[{horizontalinitials, verticalinitials, gr2, ppvector}]
]
```

Example

```
DDynamicss[{M Exp[1.1 (1 - M/.9) - .9 P],
M (1 - Exp[-2.2 P])}, M, P, .3, .4]
```

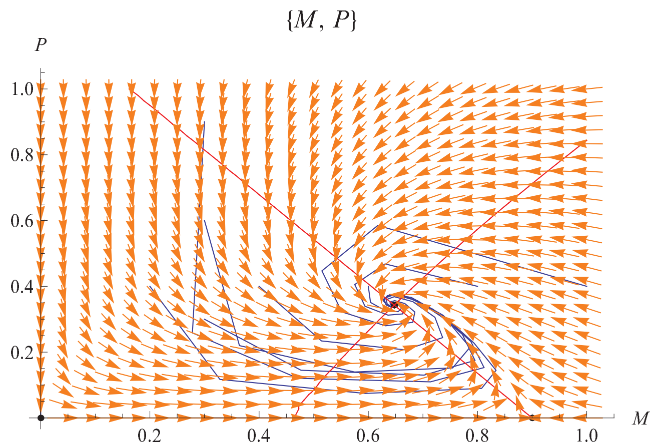

A.4 Bifurcation Diagram

Code

```
Bif2D[fg_, varx_, vary_, x0_, y0_, param_, interval_] :=
 Module[{F, G, X, Y, p0, lll},
  F[x_, y_] := fg[[1]] /. {varx -> x, vary -> y};
  G[x_, y_] := fg[[2]] /. {varx -> x, vary -> y};
  X[a_] := F[a[[1]], a[[2]]];
  Y[b_] := G[b[[1]], b[[2]]];
  p0 = {x0, y0};
  Iterasyon[d_] :=
   Nest[{X[{#[[1]], #[[2]]}], Y[{#[[1]], #[[2]]}]} &, p0, d];
  Tx := Table[Iterasyon[n][[1]], {n, 80, 87}];
  Ty := Table[Iterasyon[n][[2]], {n, 80, 87}];
  Plot[{Tx, Ty}, {param, interval[[1]], interval[[2]]},
```

```
   PlotRange -> All,
   AxesLabel -> {param, {Subscript[x, n], Subscript[y, n]}}]
  ]
```

Example

```
Bif2D[{x Exp[r (1 - x/4) - y], x (1 - Exp[-y])},
 x, y, .3, .2, r, {.3, 3}]
```

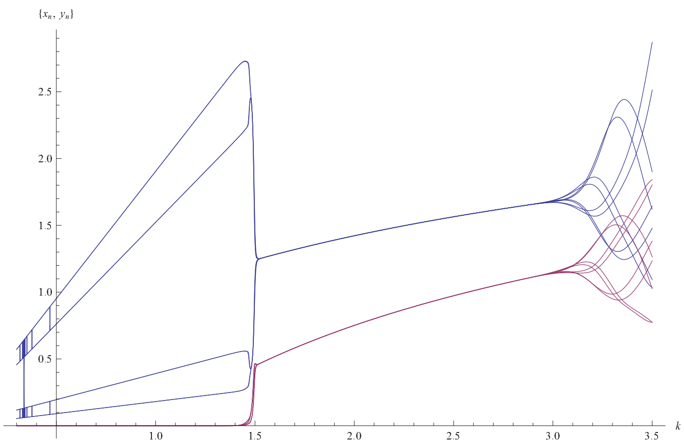

Appendix B

Stability of Fixed Points

In this section, we present the behaviour of a linear system determined by the eigenvalues and trace-determinant of the Jacobian matrix.

Table B.1: Stability of Fixed Points for 2-dimensional linear system.

Tr-Det Diagram	**Eigenvalues**	**Phase Plane**
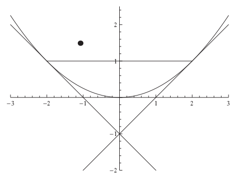	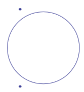	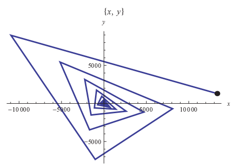
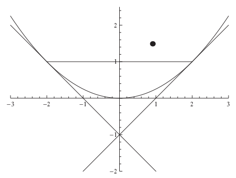	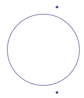	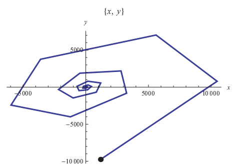
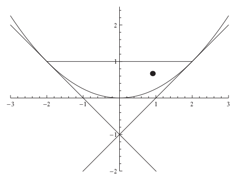	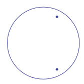	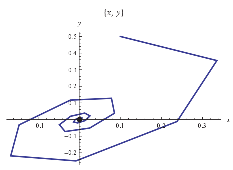
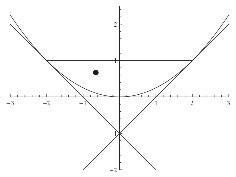	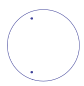	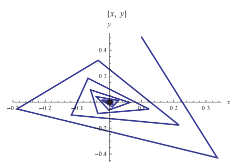
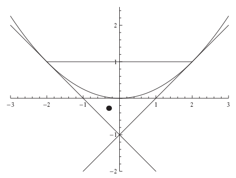	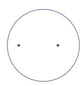	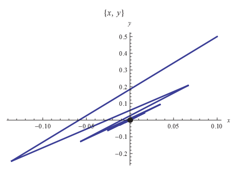
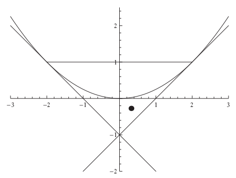	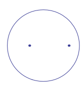	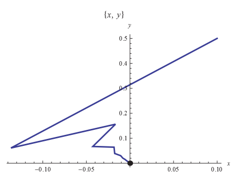

Table B.2: Stability of Fixed Points for 2-dimensional linear system.

Tr-Det Diagram	**Eigenvalues**	**Phase Plane**
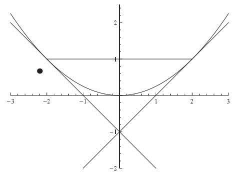	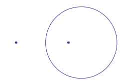	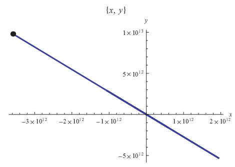
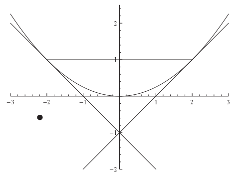	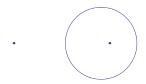	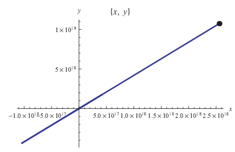
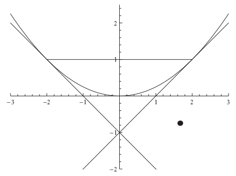	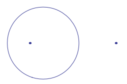	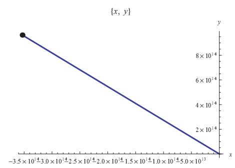
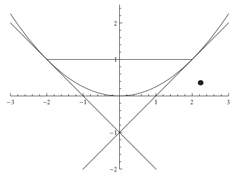	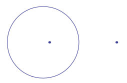	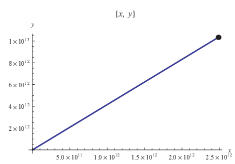
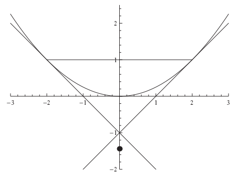	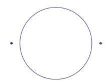	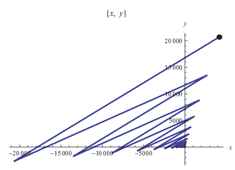
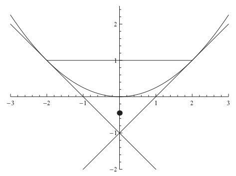	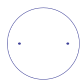	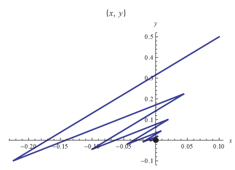

Table B.3: Stability of Fixed Points for 2-dimensional linear system.

Tr-Det Diagram	**Eigenvalues**	**Phase Plane**
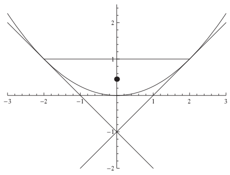	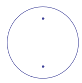	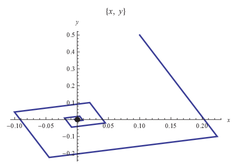
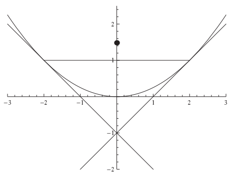	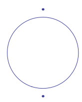	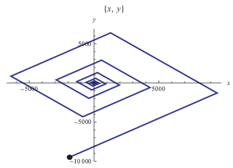
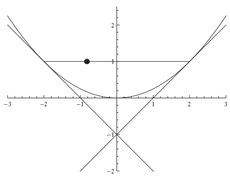	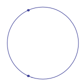	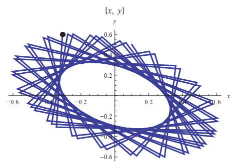
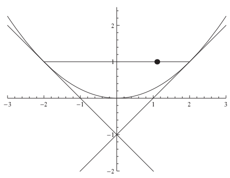	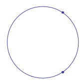	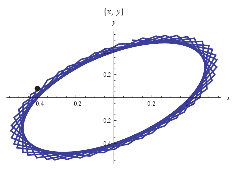
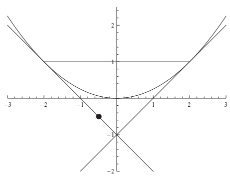	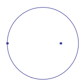	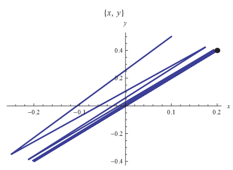
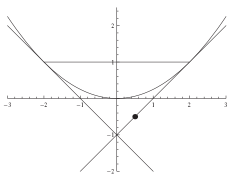	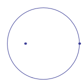	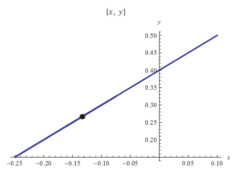

BIBLIOGRAPHY

[1] W.C. Allee, *Animal aggregation, a study in general sociology*, University of Chicago Press, Chicago, USA, 1931.

[2] W.C. Allee, *The Social Life of Animal*, William Heinemann, 1938.

[3] L. Allen, *An introduction to mathematical biology*, Prentice Hall, 2007.

[4] J.R. Beddington, C.A. Free, and J.H. Lawton, *Dynamic complexity in predator-prey models framed in difference equations*, Nature **225** (1975), 58–60.

[5] R. J. H. Beverton and S. J. Holt, *On the dynamics of exploited fish populations*, vol. 19, Chapman and Hall, 1957.

[6] X. Cabré, E. Fontich, and R. de la Llave, *The parameterization method for invariant manifolds i: Manifolds associated to non-resonant subspaces*, Indiana Univ.Math. J. **52** (2003), 283–328.

[7] J. Carr, *Application of center manifolds theory*, Applied Mathematical Sciences, Springer-Verlag, New York, 1981.

[8] H. Caswell, *Matrix population models: construction, analysis, and interpretation*, vol. 2nd, Sinauer Associates, 2001.

[9] F. Courchamp, L. Berec, and J. Gascoigne, *Allee effects in ecology and conservation*, Oxford University Press, 2008.

[10] C. Çelik, O. Duman, *Allee effect in a discrete-time predator-prey system*, Chaos, Solitons and Fractals 40, (2009) 1956-1962.

[11] M.G. Neubert and M. Kot, *The subcritical collapse of predator populations in discrete-time predator-prey models*, Mathematical Biosciences, **110**, (1992), 45–66, ISSN 0025-5564, 10.1016/0025-5564(92)90014-N.

[12] S. Elaydi, *An introduction to difference equations*, Springer, 2000.

[13] S. Elaydi, *Discrete chaos: With applications in science and engineering, second edition*, Chapman & Hall/CRC, 2008.

[14] S. Elaydi and R.J. Sacker, *Population models with allee effect: a new model*, Journal of Biological Dynamics **4** (2010), no. 4, 397–408.

[15] S. Elaydi and R. Sacker, *Basin of Attraction of Periodic Orbits of Maps on the Real Line,* Journal of Difference Equations and Applications , (2004), **10**, Iss. 10.

[16] S.A. Geritz and E. Kisdi, *On the mechanistic underpinning of discrete-time population models with complex dynamics*, J Theor Biol. (2004), no. 228, 261–9.

[17] P.H. Leslie and J. C. Gower, *The properties of a stochastic model for the predator-prey type of interaction between two species*, Biometrika, V 47, 3/4, p. 219, 1960.

[18] M. Guzowska, R. Luis, and S. Elaydi, *Bifurcation and invariant manifolds of the logistic competition model*, Journal of Difference Equations and Applications **17** (2010), no. 12, 1851–1872.

[19] J. Hofbauer and K. Sigmund, *Evolutionary games and population dynamics*, Cambridge University Press, Cambridge New York, NY, 1998.

[20] R.A. Holmgren, *A first course in discrete dynamical systems*, Springer-Verlag, New York, 1994.

[21] A.N.W Hone, M.V. Irle, and G.W. Thurura, *On the neimark–sacker bifurcation in a discrete predator-prey system*, Journal of Biological Dynamics **4** (2010), no. 6, 594–606.

[22] S.R.-J. Jang and S.L. Diamond, *A host-parasitoid interaction with allee effects on the host*, Computers and Mathematics with Applications **53** (2007), 89–103.

[23] N. Karydas and J. Schinas, *The center manifold theorem for a discrete system*, Appl. Anal. **44** (1992), 267–284.

[24] P.A. Stephens, W.J. Sutherland, and R.P. Freckleton, *What is the Allee Effect*, Oikos **87** (1999), 185-90.

[25] P.A. Stephens and W.J. Sutherland, *Vertebrate mating systems, Allee effects and conservation.* In M. Apollonio, M. Festa-Bianchet and D. Mainardi, eds. *Vertebrate mating systems*, pp. 186-213, World Scientific Publishing, Singapore, 2000.

[26] D. Clark and M. R. S. Kulenovik, *On a coupled system of rational difference equations*, Comput. Math. Appl.,(2002)

[27] M. P. Hassell and H. N. Comins, *Discrete time models for two-species competition*, Theor: Popul.Biol., 9, (1976), 202-221

[28] M.R.S. Kulenovic and M. Nurkanovic, *Global Asymptotic Behavior of a Two-dimensional System of Difference Equations Modeling Cooperation*, Journal of Difference Equations and Applications,2003 VOL. 9 (1). pp. 149-159

[29] J. C. Misra and A. Mitra, *Instabilities in Single-Species and Host-Parasite Systems:Period-Doubling Bifurcations and Chaos*, An Int. Jour. Computer and Graphics with Applications, 52, (2005), 525-538

[30] J. F. Selgrade and M. Ziehe, *Convergence to equilibrium in a genetic model with differential viability between the sexes*, J. Math. Eiol., 25 (1987), 477-490.

[31] H. L. Smith, *Monotone Dynamical Systems: An introduction to the Theory of Competitive and Cooperative Systems*, American Mathematical Society, Providence, 1995.

[32] A. Kelly, *The stable, center-stable, center-unstable and unstable manifolds*, J. Differential Equ. **3** (1967).

[33] M. Kot, M. A. Lewis, and P. Van Den Driessche, *Dispersal data and the spread of invading organisms*, Ecology **77** (1996), no. 7, 2027–2042.

[34] A.M. Kramer, B. Dennis, A.M. Liebhold, and J.M. Drake, *The evidence for allee effects*, Population Ecology **51** (2009), no. 3, 341–354 (English).

[35] Y.A. Kuznetsov, *Elements of applied bifurcation theory*, Springer, New York, 1998.

[36] M.A. Lewis and P. Kareiva, *Allee dynamics and the spread of invading organisms*, Theoretical Population Biology **43** (1993), no. 2, 141 – 158.

[37] G. Livadiotis and S. Elaydi, *General allee effect in two-species population biology*, Journal of Biological Dynamics **6** (2012), no. 2, 959–973, PMID: 22881395.

[38] A.J. Lotka, *Elements of physical biology*, Baltimore: Williams and Wilkins, 1925.

[39] R. Luís, S. Elaydi, and S. Oliveira, *Stability of ricker-type competition model and the competitive exclusion principle*, Journal of Biological Dynamics **5** (2011), 636–660.

[40] J. Marsden and M. McCracken, *The hopf bifurcation and its application*, Springer-Verlag, New York, 1976.

[41] R. M. May, *Limit cycles in predator-prey communities.*, Science **177** (1972), no. 4052, 900–902.

[42] J. D. Murray, *Mathematical biology*, Springer, New York, 2002.

[43] Ju.I. Neimark, *On some cases of periodic motions depending on parameters.*, Dokl. Akad. Nauk SSSR (1959), 129, 736–739 [in Russian].

[44] A. Nicholson and V. Bailey, *The balance of animal population*, Proceedings of the Zoological Society of London 3 (1935), 551–598.

[45] W. E. Ricker, *Stock and recruitment*, Journal of the Fisheries Research Board of Canada **11** (1954), no. 5, 559–623.

[46] R. Sacker, *On invariant surfaces and bifurcation of periodic solutions of ordinary differential equations*, Report IMM-NYU **333** (1964),New York University.

[47] E. Scheinerman, *Invitation to dynamical systems*, Prentice Hall, Upper Saddle River, N.J, 1996.

[48] P. Turchin, *Complex population dynamics : a theoretical/empirical synthesis*, Princeton University Press, Princeton, N.J, 2003.

[49] Ü. Ufuktepe and S. Kapçak, *Stability analysis of a host parasite model*, Advances in Difference Equations **79** (2013), doi:10.1186/1687-1847-2013-79.

[50] Volterra V., *Fluctuations in the abundance of a species*, Nature **118** (1924), 558–560.

[51] A. Vanderbauwhede, *Center manifolds, normal forms and elementary bifurcations*, Dynamics Reported, 1989.

[52] W-X. Wang, Y. Zhang, and C. Liu, *Analysis of a discrete-time predator-prey system with allee effect*, Ecological Complexity **8** (2011), 81–85.

[53] S. Wiggins, *Introduction to applied nonlinear dynamical systems and chaos*, Springer, New York, 2003.

[54] S-R. Zhou, Y-F. Liu, and G. Wang, *The stability of predator-prey systems subject to the allee effects*, Theoretical Population Biology **67** (2005), no. 1, 23–31.

VITA

Sinan Kapçak was born in 1978 in Diyarbakır, Turkey.

He graduated from Akdeniz University in 2001 with a degree in Mathematics. He received his Masters of Mathematics degree from İzmir Institute of Technology in 2007. He spent his 2006-2007 Fall semester at the University of Cantabria, Spain, Department of Applied Mathematics and Computational Science, studying on Petri Nets. With a Ph.D. research grant from TÜBİTAK, he studied on Discrete Dynamical Systems and Mathematical Modelling at Trinity University, USA, in the second half of 2012, under the supervision of his co-supervisor Prof. Dr. Saber Elaydi.

He completed the requirements for the Doctor of Philosophy degree in the Graduate Program of Applied Mathematics and Statistics at İzmir University of Economics under the supervision of Prof. Dr. Ünal Ufuktepe and Prof. Dr. Saber Elaydi. His research interests include Dynamical Systems and Biomathematics.